

# Cellulose in atmospheric particulate matter at rural and urban sites in Europe

Adam Brighty<sup>1,a</sup>, Véronique Jacob<sup>1</sup>, Gaëlle Uzu<sup>1</sup>, Lucille Borlaza<sup>1</sup>, Sébastien Conil<sup>2</sup>,  
Christoph Hueglin<sup>3</sup>, Stuart K. Grange<sup>3,4</sup>, Olivier Favez<sup>5,6</sup>, Cécile Trébuchon<sup>7</sup>, and Jean-Luc  
Jaffrezo<sup>1</sup>

<sup>1</sup> University Grenoble Alpes, CNRS, IRD, INP-G, IGE (UMR 5001), 38000 Grenoble, France

<sup>2</sup> ANDRA, DRD/GES Observatoire Pérenne de l'Environnement, 55290 Bure, France

<sup>3</sup> Empa, Swiss Federal Laboratories for Materials Science and Technology, Überlandstrasse 129, 8600 Dübendorf, Switzerland

<sup>4</sup> Wolfson Atmospheric Chemistry Laboratories, University of York, York, YO10 5DD, United Kingdom

<sup>5</sup> Institut national de l'environnement industriel et des risques (INERIS), Parc Technologique Alata BP2, 60550 Verneuil-en-Halatte, France

<sup>6</sup> Laboratoire Central de Surveillance de la Qualité de l'Air (LCSQA), 60550 Verneuil-en-Halatte, France

<sup>7</sup> Atmo AURA, F-38400 Grenoble, France

<sup>a</sup> now at: Centre for Environmental Policy, Imperial College London, Weeks Building, SW7 1NE

**Correspondance:** Adam Brighty (adam.brighty1@gmail.com) and Jean-Luc Jaffrezo (Jean-luc.Jaffrezo@univ-grenoble-alpes.fr)

## Abstract

The spatiotemporal variations of free cellulose concentrations in atmospheric particles, as a proxy for plant debris, were investigated using an improved protocol with an HPLC-PAD method. Filter samples were taken from nine sites of varying characteristics across France and Switzerland, with sampling covering all seasons. Concentrations of cellulose, as well as carbonaceous aerosol and other source-specific chemical tracers (e.g. Elemental Carbon (EC), levoglucosan, polyols, trace metals, and glucose) were quantified. Annual mean free cellulose concentrations within PM<sub>10</sub> ranged from  $29 \pm 38 \text{ ng m}^{-3}$  at Basel (urban site) to  $284 \pm 225 \text{ ng m}^{-3}$  at Payerne (rural site). Concentrations were considerably higher during episodes, with spikes exceeding 1150 and 2200 ng m<sup>-3</sup> at Payerne and ANDRA-OPE (rural site), respectively. A clear seasonality, with highest cellulose concentrations during summer and autumn, was

observed at all rural and some urban sites. However, some urban locations exhibited a weakened seasonality. Contributions of cellulose-carbon to total organic carbon are moderate on average (0.7 - 5.9 %), but much greater during ‘episodes’, reaching close to 20% at Payerne. Cellulose concentrations correlated poorly between sites, even at ranges of about 10 km, indicating the localised nature of the sources of atmospheric plant debris. With regards to these sources, correlations between cellulose and typical biogenic chemical tracers (polyols and glucose) were moderate to strong ( $R_s$  0.28 – 0.78,  $p < 0.0001$ ) across the nine sites. Seasonality was strongest at sites with stronger biogenic correlations, suggesting the main source of cellulose arises from biogenic origins. A second input to ambient plant debris concentrations was suggested via resuspension of plant matter at several urban sites, due to moderate cellulose correlations with mineral dust tracers,  $\text{Ca}^{2+}$  and Ti metal ( $R_s$  0.28 – 0.45,  $p < 0.007$ ). No correlation was obtained with the biomass burning tracer (levoglucosan), an indication that this is not a source of atmospheric cellulose. Finally, an investigation into the interannual variability of atmospheric cellulose across the Grenoble metropole area was completed. It was shown that concentrations and sources of ambient cellulose can vary considerably between years. All together, these results deeply improve our knowledge on the phenomenology of plant debris within ambient air.

## 1. Introduction

Ambient aerosols are a key component of our atmospheric system, with complex compositions arising from multiple sources and formation mechanisms. These airborne particles (or particulate matter, PM) have both climatic and health effects which remain poorly understood (Boucher et al., 2013). Particulate matter is made up of elemental and inorganic material, as well as a significant proportion of material of a carbonaceous nature (organic carbon, OC, and elemental carbon, EC) (Hansen et al., 1984; Birch and Cary, 1996; Putaud et al., 2004a; Yttri et al., 2007a; Franke et al., 2017). PM contains an important portion of organic matter (OM), the chemical composition of which remains largely unidentified (Putaud et al., 2010). In the majority of studies, at most 20% of the OM can be speciated and quantified at the molecular level (Alfarra et al., 2007; Michoud et al., 2021). Understanding the sources and atmospheric mechanisms of this OM fraction remains key to uncovering more knowledge of its climatic and health effects, on both local and larger scales (Nozière et al., 2015). Indeed, it has been hypothesised that our current understanding does not account for a number of hidden sources and processes of PM (Karagulian et al., 2015; Wagenbrenner et al., 2017; Klimont et al., 2017).

A large proportion of research in the last two decades has been focussed on the production of secondary organic aerosol (SOA) arising from the processing of volatile organic compounds (VOCs), or intermediate/semi-volatile ones (I/SVOCs). So far, a smaller effort has been made to account for the potential additional input from primary biological aerosol particles (PBAP – also known as Primary Biogenic Organic Aerosol, PBOA). However, the limited number of available studies show that a significant portion of OM can be associated with biogenic emissions (Liang et al., 2015; Alves, 2017; Samaké et al., 2019a). PBAP are emitted directly into the atmosphere from the source material, and are described as “solid airborne particles derived from biological organisms, including microorganisms and fragments of biological materials such as plant debris and animal dander” (Després et al., 2012). PBAP aerodynamic diameters can vary greatly based on the source: ranging from a few nanometres (e.g. viruses and cell fragments), to  $> 100\ \mu\text{m}$  (plant debris, fungal spores, pollen) (Pöschl, 2005). In terms of their atmospheric significance, some forms of PBAP have been shown to be very efficient ice nuclei and giant cloud condensation nuclei, in regions where anthropogenic sources do not dominate emissions (Rosenfeld et al., 2008; Pöschl, 2010). Biological particles have also been linked with acute respiratory effects (e.g. asthma), allergies, and cancer (Peccia et al., 2011). Estimations of global PBAP natural emissions are in the broad range of 50 – 1000 Tg/yr, highlighting the need for further studies to produce more precise estimates (Penner et al., 2001; Jaenicke, 2005). For comparison, global anthropogenic emissions of  $\text{PM}_{10}$  via road transport, amount to about 3.3 Tg/yr (Klimont et al., 2017),

Within modern field studies, characterisation of PM is simplified with the use of chemical tracers (also referred to as molecular markers) as proxy species. Such species should be persistently emitted from a given source and sufficiently stable in the atmosphere to be characterised and quantified. The use of these tracers can also lead to more constrained source apportionment calculations, owing to decreased uncertainties and a stronger statistical output, together with a better understanding of the emission processes (Waked et al., 2014; Weber et al., 2019; Borlaza et al., 2021).

Plant debris (e.g. air-dispersed seeds or plant fragments via abrasion or decomposition mechanisms) is suspected to be a major contributor to PBAP within the atmosphere (Graham et al., 2003; Winiwarer et al., 2009; Martin et al., 2010; Yttri et al., 2011b; Bozzetti et al., 2016;). However, atmospheric plant debris has received much less attention than other sources

of PBAP, such as fungal spores, and thus knowledge of plant debris is severely limited. Both cellulose and plant waxes (as n-alkanes) have been used as proxy species for atmospheric plant debris. Early studies of the fraction of plant debris (or vegetative detritus) centred around analysis of plant waxes as the proxy species (Simoneit and Mazurek, 1982; Rogge et al., 1993a; Rogge et al., 1993b). These studies have formed the basis of our work, using identifiable chemical species to supply information on insoluble components. For example, Rogge et al. (1993a) in their experiment found significant amounts of non-extractable, insoluble organic components, yet were able to identify soluble components, such as plant waxes, as chemical tracers for insoluble components, such as plant debris. Rogge et al. (1993a) found local differences in the n-alkanes observed pattern, as a function of the variability in local plant composition, whilst Simoneit and Mazurek (1982) found plant wax to be a major component of rural OC.

As scientific understanding increased, cellulose was proposed as a new chemical tracer for plant debris by Kunit and Puxbaum (1996) and has been used a tracer in several field and PMF studies since (Tenze-Kunit and Puxbaum, 2003; Sánchez-Ochoa et al., 2007; Caseiro, 2008; Yttri et al., 2011a; Yttri et al., 2011b; Bozzetti et al., 2016; Borlaza et al., 2021a). Interestingly, Kotianová et al. (2008) evaluated the use of both plant waxes and cellulose as plant debris tracers. They found a much weaker seasonal pattern with respect to cellulose concentrations, but showed plant wax/n-alkane concentrations peaked significantly during the warm summer months. The authors hypothesised that the difference between the two tracers revolved around plant waxes coming from the plant surface, whereas cellulose originating from bulk plant material. As such, atmospheric cellulose is predicted to be derived from machining and decomposition processes, and n-alkanes are emitted as part of surface abrasion mechanisms. Kotianová et al. (2008) found very good agreement in the results between the contributions of both cellulose and plant wax to PM<sub>10</sub>.

Studies of other molecular markers are more prominent, both within the primary biogenic fraction and other aerosol classes. The number of campaigns investigating measurements of atmospheric cellulose are scarce in comparison and do not sufficiently cover all ambient environments (Alves, 2017, and references therein). This remains a concern, especially considering that contributions of cellulose-derived carbon (cellulose-C) to overall organic carbon in the atmosphere can be significant during some periods of the year (Sánchez-Ochoa et al., 2007; Caseiro, 2008).

Cellulose is present as two forms within global flora: firstly as “free cellulose”, and also as cellulose embedded in lignin or hemicellulose. This portion of cellulose bound to lignin requires an additional delignification process before quantification in atmospheric PM, which requires harsh conditions and long reaction times (Gould, 1984; Kunit and Puxbaum, 1996). A conversion from free to total cellulose concentrations was created by Tenze-Kunit and Puxbaum (2003), where free cellulose was shown to contribute 72% of total cellulose abundance. This conversion presents large uncertainties, as it was developed using a very limited sample size ( $n < 10$ ). Thus, free cellulose is commonly used as the proxy species for atmospheric plant debris, over total cellulose.

Of the few previous characterisation studies to have taken place, only two have had a duration longer than one year. Regardless, some insights into the seasonal variations of cellulose concentrations have been afforded (Sánchez-Ochoa et al., 2007; Caseiro, 2008; Yttri et al., 2011a; Yttri et al., 2011b). For example, Sánchez-Ochoa et al. (2007) highlighted a pattern of cellulose concentration maxima during spring and summer at their rural background sites, excluding their maritime counterparts. This seasonal pattern, however, was found to be much weaker than other aerosol classes and showed higher winter concentrations than anticipated. Further, Caseiro (2008) found winter maxima at close to half their monitoring locations when observing from both urban and background locations. The reasons for the difference in seasonality between these two studies are likely to be owing to the differences in location and the variety of PM sizes used ( $PM_2$  to  $PM_{10}$ ) by Sánchez-Ochoa et al. (2007) compared to the consistent  $PM_{10}$  sampling used by Caseiro (2008). More long-term studies would be beneficial to understanding these geographical discrepancies.

The lack of sufficient long-term studies and clarity regarding cellulose characterisation of concentrations, seasonal cycles, sources, and emissions processes calls for further measurements. This would enable a better comprehension of the importance of this fraction of PBOA in atmospheric PM. In this study, we present a multi-seasonal investigation of cellulose concentrations alongside other chemical tracers in ambient aerosol, collected at nine sites across both France and Switzerland. The objective of the study was to investigate the seasonal and geographical variability of atmospheric cellulose across sites of varying characteristics. Contributions of cellulose to the OM fraction of PM, and correlations of cellulose with tracers of characteristic sources were also completed, alongside the creation of a biannual and triannual

dataset of cellulose concentrations at three sites within the Grenoble metropole and at ANDRA-OPE (both France), respectively. Further, a  $PM_{2.5}/PM_{10}$  intercomparison was also established. This study, with the gathering of one of the largest data bases on atmospheric cellulose with more than 1500 samples, aims to provide a better understanding of this understudied component of atmospheric PM.

## **2. Experimental**

### **2.1 Sampling Sites**

PM samples used for the present study have been collected during three distinct projects, which are described in the following. The locations of the corresponding measurement sites are presented on Fig. 1a and b, while site classifications, sampling periods, and numbers of available samples are summarised in Table 1 and Table 2.

The first measurement campaign (QAMECS) focused on the  $PM_{10}$  loading and composition at various sites within the Grenoble metropole (France), as part of the Mobil’Air air quality programme (Borlaza et al., 2021a,b). In these campaigns, three sites were monitored over two one-year periods (2017 – 2018, 2020 – 2021). As the largest metropolis in the Alps, Grenoble is home to around 450,000 inhabitants. The city itself is situated within an alpine valley: the centre is at relatively low altitude (between 200 and 600 metres above sea level) and is surrounded by multiple separate mountain ranges, namely Chartreuse (to the north), Belledonne (east) and Vercors (south and west). These ranges heavily inhibit horizontal air movement, leading to unique meteorological conditions and favouring the formation of temperature inversions, trapping pollutants within the valley, especially during winter. During this study, a  $PM_{10}$  sampling campaign was undertaken in the Grenoble metropole at three sites, each representing a different urban site typology: Les Frênes (LF, urban background), Vif (peri-urban) and Caserne de Bonne (CB, urban centre). All three sites are within 15 km of one another (Fig. 1b).

Secondly,  $PM_{10}$  and  $PM_{2.5}$  samples could be obtained from a monitoring campaign at the Observatoire Pérenne de l’Environnement (ANDRA-OPE), in northern France (<http://ope.andra.fr/index.php?>). Samples have been collected continuously for about a decade at this site (Golly et al., 2019; Borlaza et al., 2021c) but cellulose measurements were conducted and presented in this work for the years 2016, 2017 and 2020, only.  $PM_{10}$  and  $PM_{2.5}$

samples were taken on alternate days. The ANDRA-OPE site is situated 230 km east of Paris, on a rise in between lows of the Paris Basin and the mountains in the department of Les Vosges (OPE-ANDRA Atmospheric Station). It is subject to persistent westerly prevailing winds and is surrounded by significant agricultural activities but is notably distant from towns (> 25 km) and small villages (> 4 km).

Last but not least, simultaneous PM<sub>10</sub> and PM<sub>2.5</sub> filter samples were taken across five sites in Switzerland, as part of an EMPA monitoring campaign (Grange et al., 2021). These sites varied in characteristics and were sampled for one year (from June 2018 to May 2019). Two rural sites, Magadino and Payerne, are included within the study. The former is located south of the Alps, whilst the latter is found on the Northern plateau roughly 50 km from the nearest city of Bern. Filter samples were also taken from urban sites within three of the most populous cities in Switzerland: Basel, Bern and Zurich. Zurich has a similar topography to the Grenoble metropole, whilst the traffic-impacted site in Bern resides within a ‘street canyon’, thus both sites may also experience inhibited air movement. The monitoring site in Basel is within a suburban area, located in an open and park-like environment. It is not expected to be impacted by accumulation effects.

*Table 1: Sampling period and site characteristics for the PM<sub>10</sub> sampling campaign. LF = Les Frênes, CB = Caserne de Bonne. LF, CB and VIF represent sites from the Grenoble metropole.*

Site	PM Size, $\mu\text{m}$	Site Type	Sampling Start	Sampling Finish	# Samples
<b>LF</b>	10	Urban	28/02/2017	31/03/2018	286
		Background	02/01/2020	12/03/2021	
<b>Vif</b>	10	Peri-urban	28/02/2017	31/03/2018	218
			30/06/2020	12/03/2021	
<b>CB</b>	10	Urban	28/02/2017	10/03/2018	209
			30/06/2020	12/03/2021	
<b>ANDRA-OPE</b>	10	Rural background	04/01/2016	27/12/2017	174
			04/01/2020	29/12/2020	
<b>Zurich</b>	10	Urban	03/06/2018	29/05/2019	88
<b>Payerne</b>	10	Rural	03/06/2018	29/05/2019	90
<b>Basel</b>	10	Suburban	03/06/2018	29/05/2019	90
<b>Magadino</b>	10	Rural	03/06/2018	29/05/2019	90
<b>Bern</b>	10	Urban-traffic	03/06/2018	29/05/2019	89

*Table 2: Sampling period and site characteristics for the PM<sub>2.5</sub> sampling campaign*

Site	PM Size / $\mu\text{m}$	Site Type	Sampling Start	Sampling Finish	# Samples
<b>ANDRA-OPE</b>	2.5	Rural Background	01/01/2020	26/12/2020	51
<b>Zurich</b>	2.5	Urban	03/06/2018	29/05/2019	89
<b>Payerne</b>	2.5	Rural	03/06/2018	29/05/2019	90



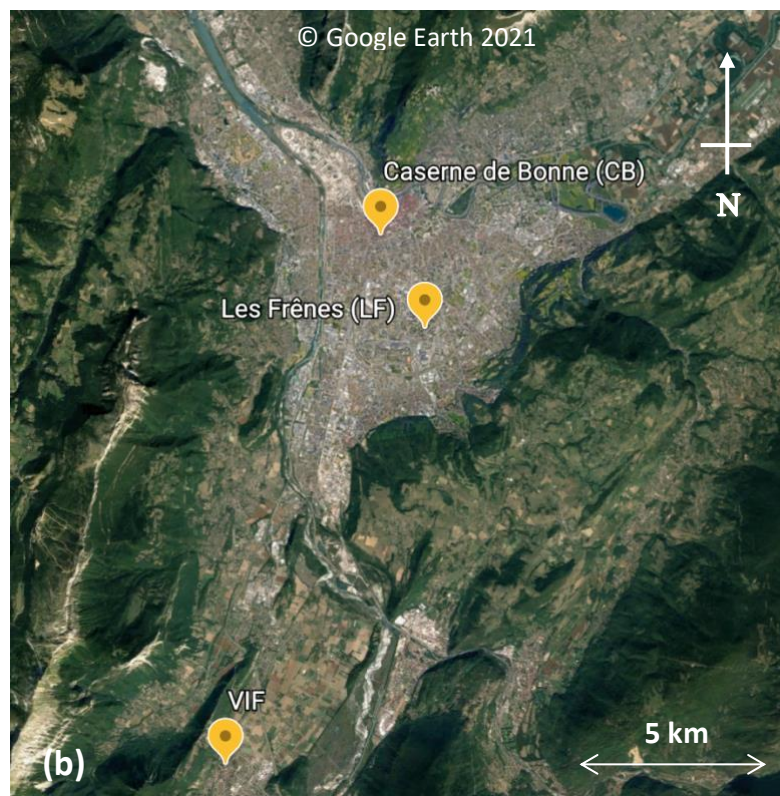
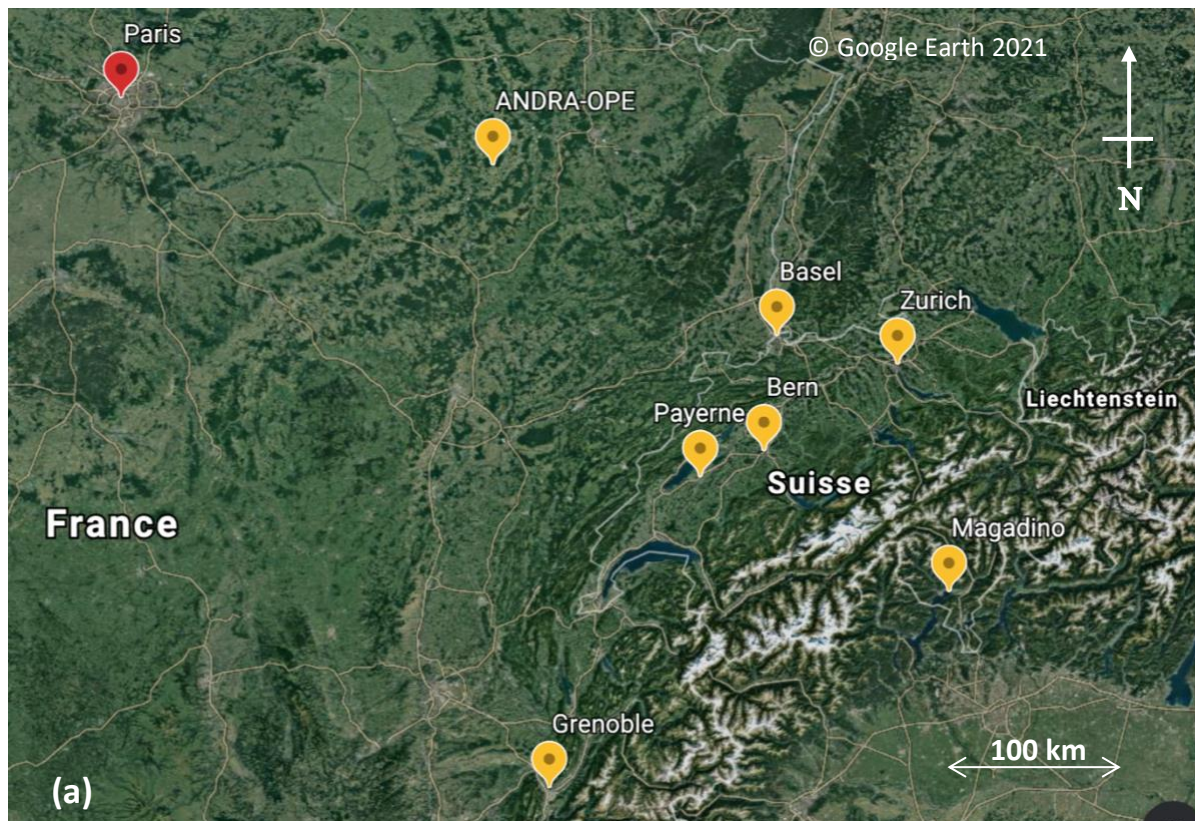


Figure 1. a) A map of all sampling sites from within the study (highlighted with yellow pin drops). Five sites are sampled within Switzerland, three sites within the Grenoble metropole, and one in Northern France – ANDRA-OPE. b) Situation of the three sampling sites within Grenoble.



## 2.2 Sampling Procedure

At each of the nine sites used for the present study, daily (24-h) PM sample collection periods were conducted according to Table 1 and Table 2 (starting at 00:00 or 09:00 local time) with an average 3-day sampling interval within the Grenoble metropole, 4-day interval for the Swiss sites, and 6-day for the ANDRA-OPE monitoring site. Additional samples for PM<sub>10</sub> were collected daily during 9 weeks in summer 2017 in OPE and Grenoble and measured for cellulose, but are not considered in this study (Samaké et al., 2020). The PM collection was performed using high volume samplers (Digitel DA80, 30 m<sup>3</sup> h<sup>-1</sup>) onto 150 mm-diameter pure quartz fibre filters (Tissu-quartz PALL QAT-UP 2500 diameter 150 mm). Excluding the Swiss sites, filters were pre-fired at 500 °C for 12 hours before use to avoid organic contamination, and all were handled under strict quality control procedures. After collection, samples were wrapped in aluminium foil or sterile parchment, sealed in Ziploc plastic bags, and stored at < 4 °C until use for chemical analyses. Blank filters were collected to determine detection limits (DL) and to check for the absence of contamination during sample transport, setup, and recovery.

## 2.3 Set of Analyses

All PM<sub>10</sub> filters from the nine monitoring locations were analysed for cellulose, while PM<sub>2.5</sub> filter samples have been analysed at three of the monitoring locations available. The PM<sub>10</sub> and PM<sub>2.5</sub> filter samples were subjected to several other chemical analyses in order to quantify their major chemical components and tracers used in this study.

### Carbonaceous Aerosol

Organic carbon (OC) and elemental carbon (EC) were analysed with a Sunset Lab analyser following the EUSAAR2 thermo-optical protocol (Hansen et al., 1984; Birch and Cary, 1996; Aymoz et al., 2007; Cavalli et al., 2010) and according to the recommendations of EN 16909 European standard. A punch of 1.5 cm<sup>2</sup> was used and automatic split time was always selected in order to differentiate between EC and OC.

### Sugar alcohols, anhydrides and glucose

Sugar anhydrides (levoglucosan, mannosan and galactosan), sugar alcohols (mannitol, arabitol and sorbitol) and glucose were analysed by High Performance Liquid Chromatography with

Pulsed Amperometric Detection (HPLC-PAD) (Waked et al., 2014; Samaké et al., 2019a). A Thermo-Fisher ICS 5000<sup>+</sup> HPLC was used with a 4 mm diameter Metrosep Carb 2×150 mm column and 50 mm pre-column in isocratic mode with an eluent of 15% of sodium hydroxide (200 mM), sodium acetate (4 mM) and 85% water, at 1 mL min<sup>-1</sup>. For this analysis, an extraction was performed upon 5.09 cm<sup>2</sup> punches soaked in 7 mL of ultra-pure water under vortex agitation for 20 minutes. The extract was then filtered with a 0.25 µm porosity Acrodisc (Milipore Millex-EIMF) filter before analysis.

#### Ionic components

Quantification of sodium (Na<sup>+</sup>), ammonium (NH<sub>4</sub><sup>+</sup>), potassium (K<sup>+</sup>), magnesium (Mg<sup>2+</sup>), calcium (Ca<sup>2+</sup>), chloride (Cl<sup>-</sup>), nitrate (NO<sub>3</sub><sup>-</sup>), sulfate (SO<sub>4</sub><sup>2-</sup>), and methane sulfonic acid (MSA) was completed using ion chromatography (IC), in agreement with EN 16913. An extraction was performed on 11.34 cm<sup>2</sup> filter punches in 10 mL of ultra-pure water under vortex agitation for 20 minutes. The extract was then filtered with a 0.25 µm porosity Acrodisc (Milipore Millex-EIMF) filter. The major ionic components were measured by ion chromatography (IC) following a standard protocol described in Jaffrezzo et al. (1998) and Waked et al. (2014) using an ICS3000 dual channel chromatograph (Thermo-Fisher) with AS11HC column for the anions and CS12 for the cations.

#### Major and trace elements

Preparation of an extract was completed via mineralisation of a 38 mm diameter filter punch in 5 mL of HNO<sub>3</sub> (70%) and 1.25 mL of H<sub>2</sub>O<sub>2</sub> at 180 °C for 30 minutes in a microwave oven (microwave MARS 6, CEM). The analysis of 18 elements (Al, As, Ba, Cd, Cr, Cu, Fe, Mn, Mo, Ni, Pb, Rb, Sb, Se, Sn, Ti, V, and Zn) was performed on each filter extract using inductively coupled plasma mass spectroscopy (ICP-MS) (ELAN 6100 DRC II PerkinElmer or NEXION PerkinElmer) akin to the method described by Alleman et al. (2010).

#### Cellulose

The concentration of “free” cellulose within the filter samples was determined following an improved protocol based on the enzymatic procedure proposed by Kunit and Puxbaum (1996). Free cellulose was extracted in an aqueous solution, which was then enzymatically hydrolysed to glucose units using two cellulolytic enzymes. The glucose concentration was then quantified by using an HPLC-PAD method. The hydrolysis step was the same as originally proposed, however the enzyme quantities and analytical step have been modified in our protocol.

First, a 21 mm diameter punch was soaked in 3 mL of aqueous solution with a thymol buffer (pH 4.8, see supplementary information) and was extracted for 40 minutes in an ultrasound bath. The two enzymes are added into the solution containing the filter: cellulase (from *Trichoderma reesei*, Sigma Aldrich, C2730) with 20  $\mu\text{L}$  of an aqueous solution at 70 units  $\text{g}^{-1}$  and glucosidase (from *Aspergillus niger*, Sigma Aldrich, 49291), with 60  $\mu\text{L}$  of an aqueous solution at 5 units  $\text{g}^{-1}$ . The filter-containing solution was then incubated at 50 °C for 24 hours for hydrolysis to occur. Hydrolysis was then terminated by denaturing the enzymes, by placing the solution in an oven at 100 °C for 45 minutes. Finally, the solution was centrifuged (9000 rpm) for 15 minutes at 15 °C and carefully separated and extracted from the filter and enzymes, before being analysed with an HPLC-PAD instrument.

The HPLC-PAD (Dionex DX500) was equipped with a Metrohm column (250 mm long, 4 mm diameter), with an isocratic run of 40 minutes with the eluents A (84%,  $\text{H}_2\text{O}$ ), B (14%, 100 mM NaOH), and C (2%, 100 mM NaOH + 150mM NaOAc). Column temperature was maintained at 30 °C. Eluent flow rate was 1.10  $\text{mL min}^{-1}$ , and injection volume was 250  $\mu\text{L}$ . Each analytical batch contained six glucose and six cellulose hydrolysis standard solutions, alongside unknown samples. Cellulose standards are used to calculate the cellulose-to-glucose hydrolysis efficiency for each batch and are made from cellulose beads of 20  $\mu\text{m}$  (Sigma Aldrich, S3504). The final calculation of the atmospheric concentration of the free cellulose takes this efficiency of conversion into account. The efficiency was variable between batches, but was typically between 75 – 94%, resulting in an average of  $85 \pm 8 \%$ . The calculation also subtracts the initial concentrations of atmospheric glucose of each sample, determined in parallel with the aforementioned analysis of sugars and polyols. Finally, field and procedural blanks are taken into account. The procedural blank results are greatly improved when the stock cellulase enzyme solution is filtered to lower their glucose content. This is performed through a series of centrifugal cleaning steps ( $n=10$ ) by tangential ultrafiltration in a Vivaspin 15R tube at 9000 rpm in Milli-Q water. Additional procedural information can be found in the supplementary information (SI).

## 2.4 Cellulose Method Validation

This cellulose quantification method was subjected to a repeatability test, in order to quantify the uncertainties with respect to glucose content within the filter punches. Briefly, a high-volume sampler (Digitel DA80, 30  $\text{m}^3 \text{h}^{-1}$ ) was used to collect  $\text{PM}_{10}$  onto a pre-fired quartz

fibre filter (Tissu-quartz PALL QAT-UP 2500 diameter 150 mm) on the roof of the laboratory, and sampled a total of 615.1 m<sup>3</sup> of air on 15/03/2021. Ten filter punches of 21 mm were then taken and subjected to the same cellulose-to-glucose enzymatic procedure as for normal samples. It is important to state that we assume constant concentrations of both native glucose and cellulose within the filter, as well as the same enzymatic cellulose-to-glucose conversion efficiency for all ten filter punches. Each filter punch was then analysed three times using the same HPLC-PAD method, to monitor repeatability in terms of both cellulose hydrolysis and PAD glucose concentration measurements. Post hydrolysis, the total glucose content of the ten filters was found. The variability (Relative Standard Deviation – RSD) was small, ranging from 0.7 – 5.7 % for the three repeats of the same filter sample. The RSD of the glucose content within the ten filter punches was calculated to be 9.9 %. For a 95% confidence in the uncertainty estimate, the uncertainty in the measurement was therefore found to be 20% at a maximum.

## **2.5 Limit of Quantification**

In order to check for potential contamination of filters during transport, sampling and storage, blank filters were taken across the nine sites. Within the Grenoble metropole, blank filters were taken at Les Frênes and then applied to Caserne de Bonne and Vif (labelled QAMECS in Table 3). Further, blank filters were taken at ANDRA-OPE on both PM<sub>10</sub> and PM<sub>2.5</sub> sampling days. With regards to the Swiss sites (EMPA), blanks were taken from each sampling site and an average glucose concentration taken from across the five locations.

Glucose concentrations calculated in the blanks were then subtracted from measured glucose concentrations within each sample. After, any sample that then yielded a negative concentration of glucose was deemed to be lower than the quantification limit (< QL), representing 5.2 % of all samples. Table 3 summarises the concentrations of cellulose on the blank filters, which has been converted from the blank glucose concentration and the average sampling volume taken across the series. QL varied according to the site, from 0.53 to 13.4 ng m<sup>-3</sup>. In subsequent analyses of monthly, seasonal or annual concentrations (sections 3.1 - 3.3 and 3.6), any sample that was deemed < QL was assigned a cellulose concentration of [Blank]/2. This prevents an artificial increase in average cellulose concentrations.

Table 3: Cellulose concentrations derived from blank filters to derive the quantification limit (QL) for each site.

Campaign	QAMECS					EMPA			ANDRA-OPE
Site	LF	CB	VIF	Basel	Bern	Magadino	Payerne	Zurich	ANDRA
Blank conc <sup>n</sup> , ng m <sup>-3</sup>	7.1	7.1	7.1	0.53	0.53	0.53	0.53	0.53	13.4
No. Field Blanks	3	3	3	5	5	5	5	5	2
No. Samples < QL	14	16	32	14	3	0	0	0	3
% Samples < QL	4.9	7.7	14.7	15.6	3.4	0	0	0	1.7

### 3. Results and Discussion

In the following, cellulose concentrations are reported as “free” cellulose. The multiplication factor of 1.39 derived by Tenze-Kunit and Puxbaum (2003) could have been used to derive “total” cellulose. We chose not to do this, due to the large uncertainty in this ratio. From this point onwards, “free” cellulose will be regarded as cellulose.

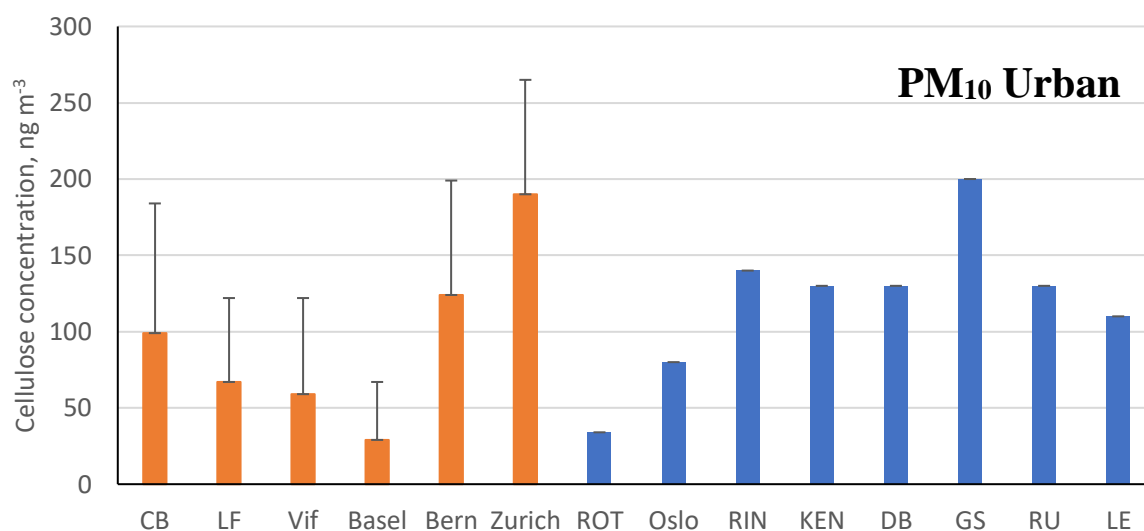
#### 3.1 Comparison with previous data from the literature

Figure 2 illustrates the annual averages of cellulose concentrations across our nine sites (in orange), as well as previous data from the literature (in blue), sorted by site typology and sampled particle size. The bars represent either annual cellulose averages (if sampling lasted greater than one year) or cellulose averages for the designated sampling period. We believe that the roughly 4440 samples (excluding the ones produced within our study) considered in this literature survey represent the near complete data base of cellulose concentrations in PM available in the literature. A tabulated version of the results from within the study can be found in Table 4. An expanded version of Table 4, also including previous literature results, can be found in Table S1 (SI). The evolution of cellulose concentrations across the respective sampling periods for our study have further been included in the SI (Fig. S1).

The concentrations measured in this study are in the same order of magnitude as those reported in the literature for previous measurement campaigns. This is generally the case for both seasonal averages and overall maximum concentrations, in both coarse and fine mode aerosol (Sánchez-Ochoa et al., 2007; Caseiro, 2008; Yttri et al., 2011a; Yttri et al., 2011b). As shown in Fig. 4, annual cellulose concentrations in PM<sub>10</sub> in our study ranged from  $29.3 \pm 38.4$  ng m<sup>-3</sup> (Bern) to  $284.3 \pm 224.8$  ng m<sup>-3</sup> (Payerne), and in PM<sub>2.5</sub> ranged from  $15.9 \pm 15.0$  ng m<sup>-3</sup>

(ANDRA-OPE) to  $118.1 \pm 76.5 \text{ ng m}^{-3}$  (Payerne). This annual average  $\text{PM}_{10}$  cellulose concentration taken at Payerne is higher than any previously recorded in literature by roughly  $50 \text{ ng m}^{-3}$ .

Moreover, results obtained at Payerne evidenced three episodic (high cellulose concentration) spikes (03/06, 13/07, and 29/07 – highlighted in red, Fig. S1) which exceeded any maximum episode found in literature, by at least  $160 \text{ ng m}^{-3}$  (Sánchez-Ochoa et al., 2007; Caseiro, 2008; Winiwarter et al., 2009). One striking feature of the overall concentration evolution at Payerne is the high cellulose concentrations at the beginning in June 2018, and the surprisingly low concentrations in April and May 2019 (Fig. S2). Another high concentration episode exceeding those found in literature was documented at the rural site of ANDRA-OPE. The episodic concentration of  $2027 \text{ ng m}^{-3}$  (07/07/2018 – highlighted in red, Fig. S1) is almost double that of any other measurement, including those generally obtained in the present study. Samaké et al., (2020) recently reported at the same site a noticeable increase in concentrations of PBAP tracers, cellulose included, during harvest in the late summer 2017. However, given the concentration spike in 2018 originated during early July, the middle of the European summer, it is not sure that this new episode can be correlated with agricultural activity.





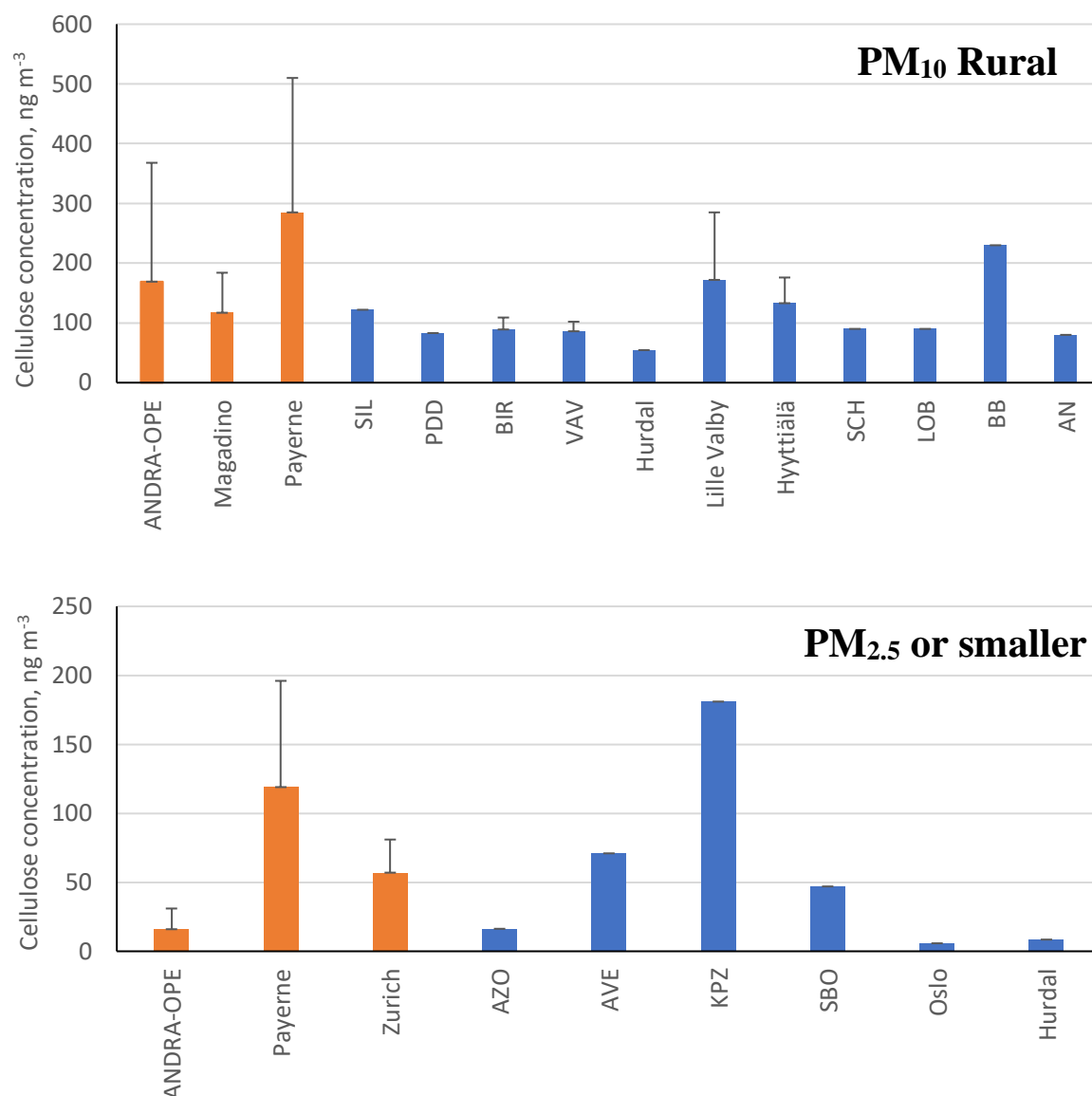


Figure 2: Annual cellulose concentrations ( $\text{ng m}^{-3}$ ) reported within this study (orange bars) alongside previous literature measurements (blue bars). Black bars represent the standard deviation of the results. Bar charts are assigned as follows: Top – urban-based sites; Middle – rural-based sites; Bottom –  $\text{PM}_{2.5}$  cellulose measurements (fine mode) or smaller. **Note: Only positive error bars are used for clarity.**

#### Countries for literature sampling sites:

**PM<sub>10</sub> Urban:** ROT – Netherlands; Oslo – Norway; RIN, KEN, DB, GS, RU and LE – Austria.

**PM<sub>10</sub> Rural:** SIL – Germany; PDD – France; BIR, Hurdal and Hyytiälä – Norway; Lille Valby, VAV – Denmark; SCH, LOB, BB and AN – Austria.

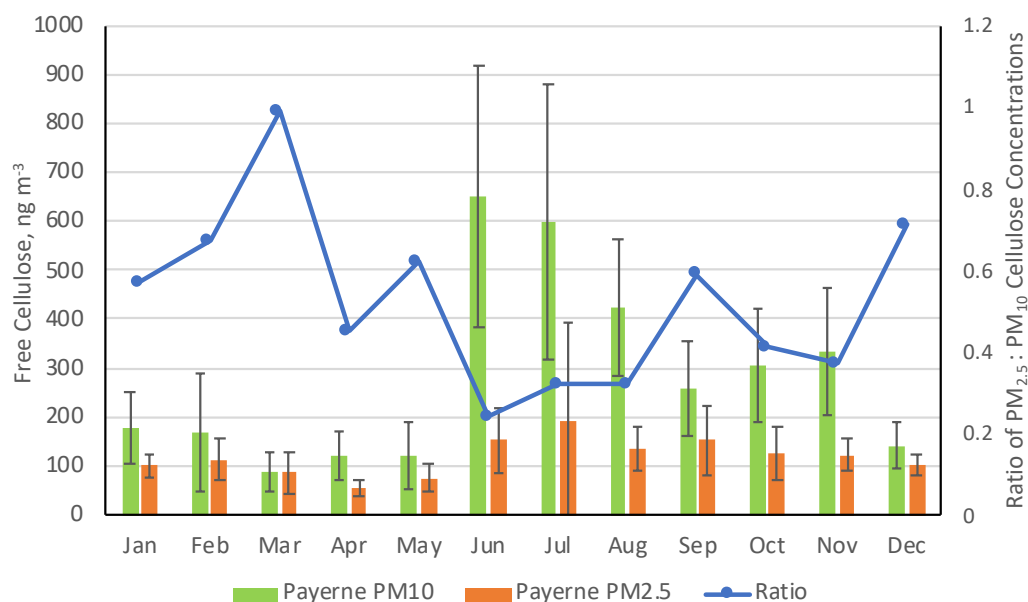
**PM<sub>2.5</sub> or smaller:** AZO, AVE – Portugal; KPZ – Hungary; SBO – Austria; Oslo, Hurdal – Norway.

Table 4: Cellulose concentrations (ng m<sup>-3</sup>) within PM<sub>10</sub> and PM<sub>2.5</sub> across the nine locations studied. Concentrations are shown as annual and seasonal overages (plus 1σ), as well as the total range of cellulose concentrations seen across the respective period.

Cellulose (ng m <sup>-3</sup> )		Annual			Winter			Spring			Summer			Autumn		
Site	Particle Size (μm)	# Samples	Mean ± SD	Range	Mean ± SD	Range	Mean ± SD	Range	Mean ± SD	Range	Mean ± SD	Range	Mean ± SD	Range	Mean ± SD	Range
LF	10	286	67 ± 55	(1 – 379)	34 ± 29	(1 – 146)	57 ± 44	(1 – 214)	98 ± 58	(29 – 379)	93 ± 60	(1 – 333)				
VIF	10	218	59 ± 63	(0.0 – 344)	43 ± 47	(0.0 – 222)	44 ± 38	(3 – 186)	68 ± 87	(1 – 344)	77 ± 65	(1 – 286)				
CB	10	206	99 ± 85	(1 – 701)	85 ± 111	(1 – 701)	131 ± 56	(46 – 288)	94 ± 59	(3 – 238)	95 ± 85	(3 – 357)				
ANDRA-OPE	10	174	169 ± 199	(3 – 2027)	90 ± 115	(3 – 518)	102 ± 116	(12 – 560)	247 ± 260	(7 – 2027)	90 ± 67	(13 – 290)				
ANDRA-OPE	2.5	51	16 ± 15	(0.3 – 41)	17 ± 21	(0.3 – 41)	< LD	< LD	15 ± 12	(6 – 32)	16 ± 18	(2 – 40)				
Basel	10	90	29 ± 38	(2 – 266)	27 ± 57	(2 – 266)	35 ± 37	(10 – 154)	32 ± 35	(11 – 179)	23 ± 16	(3 – 83)				
Bern	10	89	124 ± 75	(25 – 318)	66 ± 45	(30 – 159)	76 ± 52	(25 – 241)	143 ± 45	(99 – 306)	138 ± 72	(78 – 318)				
Magadino	10	90	117 ± 67	(16 – 348)	53 ± 23	(17 – 103)	84 ± 48	(43 – 282)	135 ± 65	(60 – 348)	131 ± 54	(48 – 279)				
Payerne	10	90	284 ± 225	(53 – 1194)	163 ± 84	(90 – 437)	108 ± 54	(53 – 284)	553 ± 246	(235 – 1194)	300 ± 114	(96 – 538)				
Payerne	2.5	90	118 ± 77	(29 – 678)	105 ± 29	(71 – 201)	74 ± 33	(29 – 163)	161 ± 122	(75 – 678)	132 ± 52	(74 – 275)				
Zurich	10	88	190 ± 75	(7 – 521)	189 ± 48	(116 – 342)	177 ± 51	(81 – 260)	197 ± 71	(7 – 330)	198 ± 112	(48 – 521)				
Zurich	2.5	89	57 ± 24	(11 – 163)	52 ± 16	(31 – 89)	52 ± 26	(13 – 199)	58 ± 20	(33 – 109)	64 ± 31	(11 – 163)				

### 3.2 Size distribution (PM<sub>10</sub> vs PM<sub>2.5</sub>)

Figure 3 presents the comparative monthly average concentrations of cellulose in PM<sub>10</sub> and PM<sub>2.5</sub> taken at the three sites of Payerne, Zurich, and ANDRA-OPE, respectively (overall concentration evolutions presented in Fig. S2, SI). Cellulose concentrations in PM<sub>10</sub> are consistently much higher than those in PM<sub>2.5</sub>, with annual average in PM<sub>2.5</sub> representing between 18 and 42 % of that in PM<sub>10</sub> for the 3 sites. However, very large fluctuations in this monthly ratio can be observed, particularly for the two rural sites (Payerne and ANDRA-OPE). This is primarily due to changes in PM<sub>10</sub> cellulose concentrations, as those within PM<sub>2.5</sub> remained largely consistent. Further, considering the overall evolution in Fig. S2, episodic PM<sub>2.5</sub> concentrations still generally remain well below the PM<sub>10</sub> cellulose concentrations around the same period. It seems that some process is largely impacting the source strength of atmospheric plant debris within PM<sub>10</sub>, particularly in the rural sites. In the city of Zurich, the cellulose PM<sub>2.5</sub>/PM<sub>10</sub> ratio remained relatively constant, just like the concentrations themselves. The comparatively low cellulose concentrations at ANDRA-OPE for 2020 (both PM<sub>10</sub> and PM<sub>2.5</sub>) are discussed as part of section 3.7, in the interannual comparison. No ratio is provided at ANDRA-OPE as PM<sub>2.5</sub> and PM<sub>10</sub> measurements were completed on different days, as opposed to simultaneous PM<sub>10</sub> and PM<sub>2.5</sub> sampling at Payerne and Zurich.



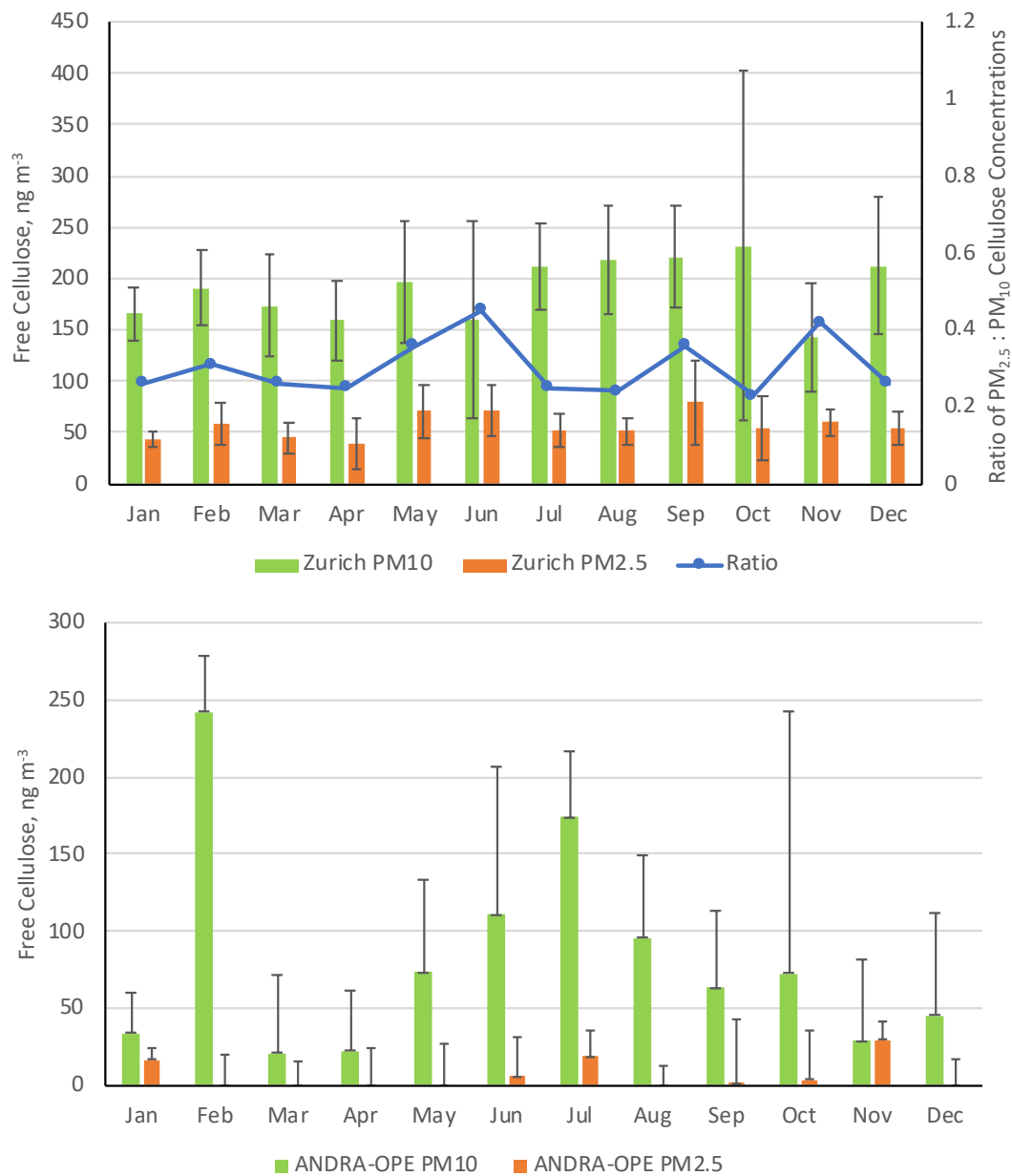


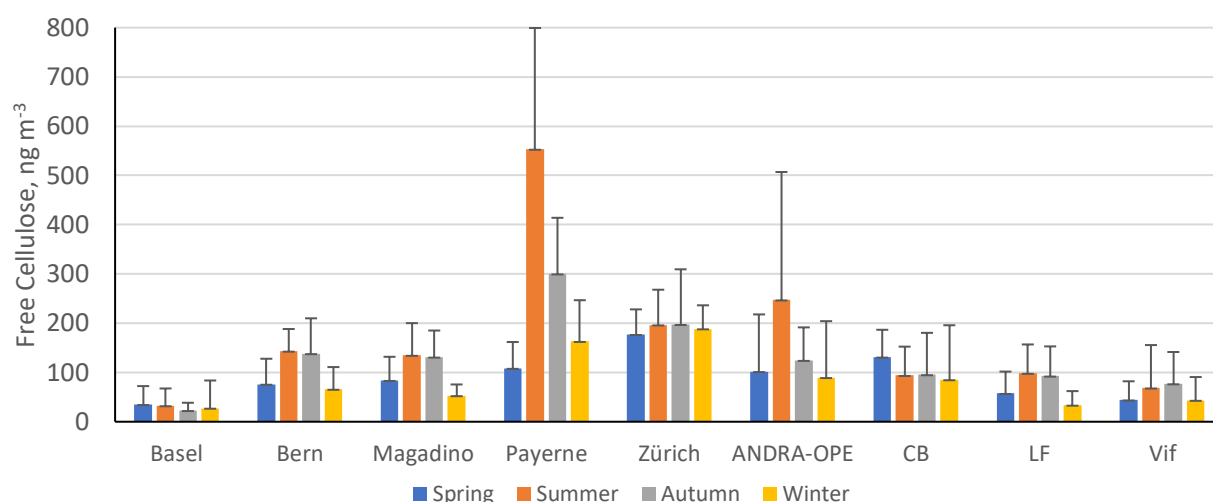
Figure 3: Monthly averages of cellulose concentrations within PM<sub>10</sub> (green bars) and PM<sub>2.5</sub> (orange bars) at the three sampling sites of Payerne (rural, top), Zurich (urban, middle) and ANDRA-OPE (rural, bottom). Black error bars represent one standard deviation of the results. The corresponding blue lines represent the ratio of the monthly mean cellulose concentrations in PM<sub>2.5</sub> : PM<sub>10</sub>. **Note: ANDRA-OPE data is only for the year of 2020, and only positive error bars are used for clarity (StDev larger than mean).**

414 Importantly, across the three sites, less than 30% of atmospheric cellulose was found within  
 415 PM<sub>2.5</sub>, on average. This large data set of size resolved cellulose concentrations confirms that  
 416 plant debris predominantly resides within the coarse aerosol mode (Sánchez-Ochoa et al., 2007;  
 417 Yttri et al., 2011a). Thus, the remainder of this work will solely discuss PM<sub>10</sub> data to understand  
 418 atmospheric cellulose and its behaviour.

### 3.3 Variations of cellulose concentrations in time and space

Previous studies indicate either a temporal variation with cellulose concentration maxima during the spring and summer seasons (Sánchez-Ochoa et al., 2007), or show very minimal seasonality (Caseiro, 2008). The following discussion will take these observations into account by presenting the results in terms of seasonal averages. Seasons were defined in three-month periods: Dec – Feb (Winter), Mar – May (Spring), Jun – Aug (Summer), Sep – Nov (Autumn). At the nine sites investigated, our PM<sub>10</sub> cellulose measurements were above the limit of detection across all seasons. Figure 4 illustrates these seasonal cellulose concentrations (ng m<sup>-3</sup>) for the nine locations. Numerical values of seasonal means and ranges are tabulated as part of Table S1 (SI).

In general, the seasonal pattern exhibited here shows higher cellulose concentrations during summer and autumn, likely due to increased temperature and humidity increasing the activity of soil and litter decomposers as well as improving the quality of the litter composition. For example, nitrogen content of leaves is shown to be greater in warmer temperatures, which leads to better conditions for leaf degradation by microbial action (Liu et al., 2006; Verma et al., 2018). It should be stated that this hypothesis would require further experiments, including specific field measurements linking soil and litter state and plant debris emission. The general trend above is exhibited at all rural sites, and some urban locations (Bern, LF, Vif). However, the extent to which these concentrations exceed the other seasons varied greatly. Normalised seasonal concentrations for each site can be found in Fig. S3, to show this variability. Considering this general seasonality, a summer-autumn maximum in cellulose concentrations deviates from the spring-summer maximum suggested by Sánchez-Ochoa et al. (2007). This may be a result of the different particle size fractions measured as part of their sampling campaign (i.e., PM<sub>2</sub>, PM<sub>2.5</sub> or PM<sub>10</sub>), compared to the consistent PM<sub>10</sub> measurements used in this study. This might also be due to the presence of three high altitude, mountainous sites comprised within the six sites investigated by Sánchez-Ochoa et al. (2007). Large standard deviations are also noticed at the two rural sites of ANDRA-OPE and Payerne, especially during the summer months. This implies a significant variability in the source of atmospheric cellulose at these sites, especially when compared to the more urban locations showing smaller standard deviations and therefore a smaller flux from the cellulose source.



Site	LF	CB	VIF	Basel	Bern	Magadino	Payerne	Zurich	ANDRA-OPE
Classification	Urban Background	Urban centre	Peri-urban	Suburban	Urban-traffic	Rural	Rural	Urban	Rural background

Figure 4: Mean cellulose concentrations ( $\text{ng m}^{-3}$ ) at each site, by season: spring (blue), summer (orange), autumn (grey) and winter (yellow). Black error bars represent one standard deviation of the seasonal averages. Only positive error bars are added, for clarity. **Note:** LF = Les Frênes; CB = Caserne de Bonne. Grenoble-based sites represented by CB, LF and Vif.

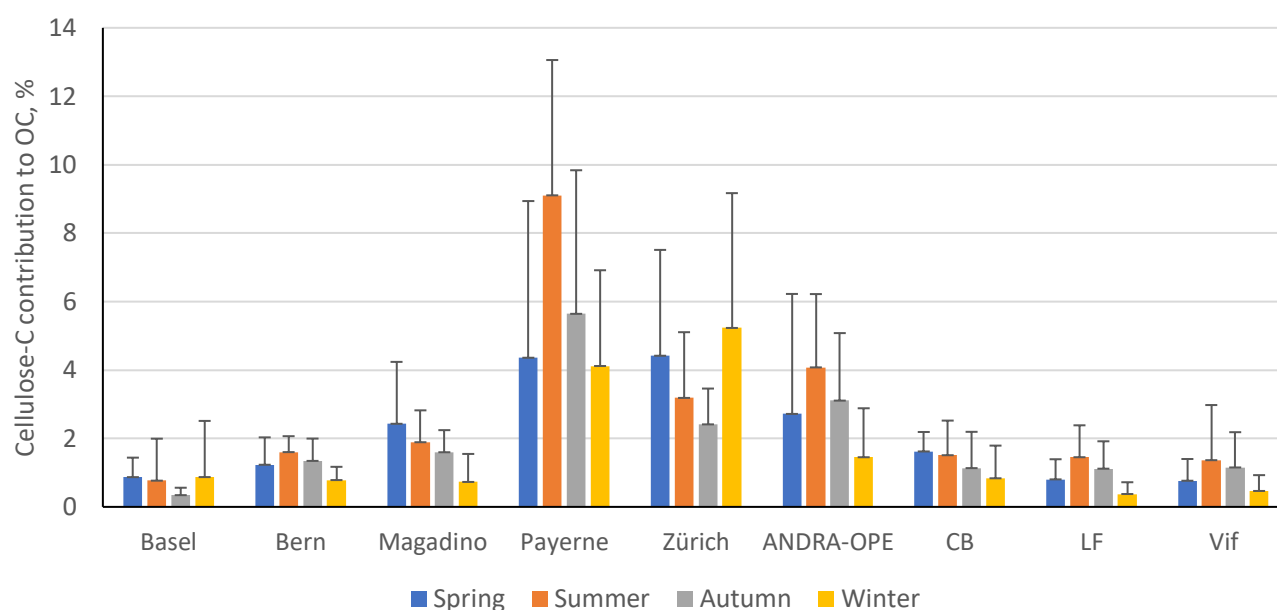
Whilst this is the general case, there are notable exceptions. Both the urban centres of Zurich and CB show very little seasonal variability compared to their more rural counterparts. Cellulose concentrations in Basel (suburban) also show minimal seasonality, but this may be due to concentrations being too small to exhibit a full seasonal pattern. This is surprising, given the close proximity of the site to a park-like area with trees and gardens. The lack of seasonality in urban settings, however, is consistent with the findings of Caseiro (2008). Additionally, Caseiro (2008) provided some evidence of cellulose concentrations at urban sites being greater than for nearby rural or background sites, with residential areas being an intermediate case. Within our Grenoble-based dataset as a comparison, CB (urban) does indeed exhibit cellulose concentrations marginally higher than the urban background site of LF and significantly higher than Vif (peri-urban).

Alongside Basel, Caserne de Bonne also deviates from the general trend of summer-autumn maxima in cellulose concentrations observed across the other seven locations investigated here. Reasons for this are unclear, but this is suggestive of a source change in atmospheric plant debris, or an additional source being present at some urban locations, that may mask the typical seasonality. Given that these locations are urban in character, the weak seasonal variations may be owing to anthropogenic activity. This will be investigated in section 3.5.



### 3.4 Contribution of Cellulose-C to OC

To determine the overall importance of cellulose contribution to PM, the percentage contribution of cellulose-carbon to total organic carbon (Cellulose-C to OC) was determined. Figure 5 illustrates this seasonal average percentage contribution. Table S3 summarises numerically the overall average and seasonal percentage contributions and the ratio of cellulose-C contribution during winter and summer. Also highlighted is the maximum contribution of cellulose-C to OC experienced over the respective sampling periods at each site.



Site	LF	CB	VIF	Basel	Bern	Magadino	Payerne	Zurich	ANDRA-OPE
Classification	Urban Background	Urban centre	Peri-urban	Suburban	Urban-traffic	Rural	Rural	Urban	Rural background

Figure 5: Seasonal contributions of cellulose-C to OC (%) in PM<sub>10</sub> across the nine sites. Seasons are as follows: Spring (blue) - Mar-May; Summer (orange) - Jun-Aug; Autumn (grey) - Sep-Nov; Winter (yellow) - Dec-Feb. Black error bars represent one standard deviation of the mean values. Only positive error bars are included, for clarity. **Note:** LF = Les Frênes, CB = Caserne de Bonne. Grenoble-based sites represented by CB, LF and Vif.

The highest contributions to OC were typically found at rural sites, potentially due to fewer local sources of OC in rural sites compared to more urban locations. In fact, the annual contribution to OC found at Payerne ( $5.9 \pm 4.4$  %) is the highest found in literature. However, the annual average for the urban site of Zurich is also in a high range, at  $3.8 \pm 2.9$  %. Regarding seasonal contributions, the rural sites in this study show a significantly different seasonal pattern compared those found in the study by Sánchez-Ochoa et al. (2007). Here, we see a noticeably smaller contribution of cellulose-C to OC during winter compared to summer. This

is reflected in the respective winter/summer ratios of cellulose-C contribution: the values in this study range between 0.36 – 0.45, in comparison to 4.2 and 0.3 at the PM<sub>10</sub> rural and high-altitude sites used in their study (Sánchez-Ochoa et al., 2007).

While seasonal contributions appear to be moderate in most cases, the contribution of cellulose-C within episodes can be much more significant. It is also worth noting that these contributions to OC are derived from free cellulose concentrations. Thus, the contribution to overall OC will be higher when considering total cellulose. At sites with typically lower seasonal contributions (Basel, Bern, LF), the episodic contributions reached between roughly 4.1 to 6.3 %. However, at the sites that illustrated a much higher seasonal average contribution to OC, the maximum contributions during episodes were found to be between 16.1 % at Zurich and 19.7 % at Payerne. These maximum contributions (detailed in Table S3) are similar to those found at the background sites by Sánchez-Ochoa et al. (2007). These values stand to highlight the substantial contribution that atmospheric plant debris can have on atmospheric composition. In other words, PBAP, and plant debris in particular, can contribute greatly to OM and must be considered within all future characterisation and source apportionment studies.

Lastly, the contribution of coarse mode (PM with diameter less than 10 µm and greater than 2.5 µm) cellulose-C to coarse mode OC was evaluated at the three sites that completed both PM<sub>10</sub> and PM<sub>2.5</sub> analysis (ANDRA-OPE, Payerne and Zurich). This can be seen in Table S4, in the SI. As PM<sub>2.5</sub> data for ANDRA-OPE was only available for the 2020 sampling campaign, PM<sub>10</sub> data from 2016 and 2017 was excluded. Table S4 shows a contribution of coarse cellulose-C to be 3.16% at ANDRA-OPE, which is of very similar magnitude to that of the overall cellulose-C contribution to OC. This is potentially due to the significant reduction in cellulose source strength at the ANDRA-OPE site during the year of 2020, compared to the years prior. This will be discussed in section 3.7. However, at both Payerne and Zurich, the annual contributions to coarse OC are notably higher (11.02 % and 13.04 %, respectively) than that of overall cellulose-C to OC (5.88 % and 3.76 %, respectively). From this data, we can see that plant debris makes up a significant component of the coarse fraction of OM within these two datasets.

### 3.5 Investigation of cellulose emission sources

To further evaluate the potential sources of plant debris into the atmosphere, correlations between cellulose and other source-specific tracers were investigated. This is the first cellulose field study to investigate these correlations with other tracers. Briefly, three specific sources have been hypothesised in the literature: direct biogenic emissions, unpyrolysed cellulose during domestic biomass burning, and anthropogenic resuspension and milling of plant debris (Sánchez-Ochoa et al., 2007; Caseiro, 2008; Yttri et al., 2011a; Yttri et al., 2011b). The chemical tracers used as proxies for these sources in this study are i) glucose and polyols, ii) levoglucosan, and iii) EC, Ca<sup>2+</sup> and Ti, respectively. A suite of correlation coefficients (Spearman's rank correlation, *R<sub>s</sub>*) was created for each site to monitor variations in correlations between site types using daily samples. Spearman's rank correlation was used in this section to better account for anomalous results between different datasets (e.g. cellulose vs polyols). A value of 1 indicates a perfect positive correlation, and a value of -1 indicates a perfect negative correlation. Table 5 shows the strength of the cellulose-tracer correlation at individual sites across the entire sampling period. A full table, inclusive with the number of data points (n) and p values for each correlation, plus *R<sub>s</sub>* values within each season, can be found in the SI (Table S5).

*Table 5: Spearman correlations (*R<sub>s</sub>*) between cellulose and characteristic chemical tracers across the nine sites. A red cell indicates a positive correlation between cellulose and the selected chemical tracer, whilst a blue cell indicates a negative correlation. A colour-coded key of corresponding *R<sub>s</sub>* values is to the right of the table. Grenoble-based sites: CB – Caserne de Bonne, LF – Les Frênes and Vif. **Note: polyols = sum of arabitol, mannitol and sorbitol.***

<i>R<sub>s</sub></i>	CB	LF	Vif	Basel	Bern	Magadino	Payerne	Zurich	ANDRA-OPE	
Polyols	0.28	0.60	0.42	0.33	0.61	0.78	0.68	0.43	0.66	1.00
Glucose	0.28	0.57	0.48	0.39	0.63	0.66	0.71	0.43	0.58	0.66
Levoglucosan	-0.06	-0.38	-0.08	0.00	-0.07	-0.37	-0.18	-0.03	-0.43	0.33
EC	0.19	-0.08	0.04	0.34	0.25	-0.03	0.07	0.25	0.11	0.00
Ca <sup>2+</sup>	0.14	0.28	0.12	0.37	0.45	-0.12	0.21	0.29	0.33	-0.33
Ti	0.28	0.34	0.03	0.40	0.39	0.05	0.31	0.31	0.18	-0.66
										-1.00

Site	LF	CB	VIF	Basel	Bern	Magadino	Payerne	Zurich	ANDRA-OPE
<b>Classification</b>	Urban Background	Urban centre	Peri- urban	Suburban	Urban- traffic	Rural	Rural	Urban	Rural background

### Biogenic sources

The best understood chemical tracers for biogenic emissions are polyols (sum of arabitol, sorbitol and mannitol) and glucose (Bauer et al., 2008; Zhang et al., 2010; Després et al., 2012).

Glucose is the most abundant monosaccharide amongst vascular plants, is an important carbon source for bacteria and fungi, and remains stable in the atmosphere (Jia et al., 2010; Zhu et al., 2015). Its multiple biological sources into the atmosphere means that it can provide a good insight as to whether atmospheric plant debris comes from a predominantly biogenic source. Polyols are also used to provide tracer correlations with cellulose. These species are typically used as markers of airborne fungi but have also been found to be present within leaves and pollen (Medeiros, 2006).

As we can see in Table 5, relatively strong positive correlations arise between cellulose and the two selected biogenic source tracers at most sites. The strongest correlations were seen at rural locations (Magadino, Payerne and ANDRA-OPE,  $p < 0.0001$ ). However, Bern and LF, traffic-impacted and urban background sites respectively, also showed similar  $R_s$  magnitudes to their rural counterparts ( $p < 0.0001$ ). This indicates that similar factors promote the emission of all of cellulose, polyols and glucose. The remaining four sites, all urban in character, showed weaker correlations of cellulose with both glucose and polyols. It should also be said that correlations across all sites were of similar magnitude when comparing cellulose-glucose and cellulose-polyol concentrations. The stronger correlations at the rural sites indicate that a significant portion of atmospheric cellulose, and thus plant debris, arises from biogenic sources at these sites. As the values are typically below 0.7, this could suggest a different timing of emissions between biogenic tracers and cellulose (e.g. meteorological conditions favouring emission of fungal spores before plant debris). This is a distinct possibility, given that sampling ranges between 3-6 days at the nine locations. Additionally, these moderate correlations with biogenic tracers could be due to some input from other sources, but of a lower magnitude. By contrast, the weaker correlations observed at most urban sites suggest that there remain other, potentially more prominent, sources at play that determine atmospheric cellulose concentrations. The two exceptions to this, LF and Bern, show that the sources of atmospheric plant debris are not consistent within each designated site type.

It is noteworthy that the five locations that illustrate the strongest correlations with glucose and polyols are the five out of the six sites in which the common, general-case seasonality is observed. It is thus likely that this typical seasonality pattern is observed where the biogenic source of plant debris is the most dominant.

## **Biomass Burning**

A potential second source of atmospheric cellulose was proposed by Sánchez-Ochoa et al. (2007) to account for anomalous high cellulose concentrations during winter. They suggested that they were caused by unburned cellulose during biomass burning (Sánchez-Ochoa et al., 2007). They also concluded that it was an unlikely process, based on the work of Schmidl et al. (2005) illustrating that only a very small concentration of cellulose can be found in wood smoke. Nevertheless, correlations between cellulose and levoglucosan, a chemical tracer for biomass burning, were completed here to provide a more robust understanding of the viability of this hypothesis (Giannoni et al., 2012; Madsen et al., 2018).

Table 5 indicates cellulose-levoglucosan tracers across all sites show no correlation with one another, and in some instances show a moderate anti-correlation ( $R_s$  -0.43 – 0.00,  $p$  0.0001 – 0.98). Stronger anti-correlations were seen at sites that also showed strong correlations with biogenic tracers. Given that the theory was based on a winter-time source of atmospheric cellulose via biomass burning, it is important to view the seasonal correlations to gain a fuller understanding (Table S5, SI). Of all sites, the Grenoble-based locations (Caserne de Bonne, Les Frênes and Vif) were the only three to have greater than the thirty data points of simultaneous cellulose and levoglucosan measurements needed for a robust correlation. None of these three locations showed any correlation between cellulose and levoglucosan ( $R_s$  0.05 – 0.18,  $p$  0.14 – 0.74). In fact, the remaining six locations showed also very weak correlation, except for the site of Bern, which showed a moderate correlation ( $R_s$  0.49,  $p$  < 0.03). But, as already mentioned, the relatively small wintertime dataset for these six other sites ( $n$  = 21 to 25) does not provide strong confidence in these results. Thus, we can state that the sources of atmospheric plant debris, as indicated by measurements of free cellulose, do not seem to include any significant input from biomass burning from domestic wood. Further investigation would be needed concerning possible emissions of total cellulose (included the one still embedded in lignin).

## **Other anthropogenic sources**

It has also been hypothesised that others anthropogenic activities may contribute to atmospheric cellulose. Caseiro (2008) noticed typically higher cellulose concentrations in urban locations, compared to the more rural ones within their study. The predominant

hypotheses for anthropogenic input of plant debris into the atmosphere were mechanisms such as resuspension via road traffic, paper usage, and lawn mowing. To test these hypotheses, correlations were computed between cellulose and known chemical tracers for man-made emissions and mineral dust: Elemental Carbon (EC) and  $\text{Ti}/\text{Ca}^{2+}$ , respectively. EC is a known primary product of combustion processes and is dominated by anthropogenic sources, including road traffic, in urban areas (Wu and Yu, 2016).  $\text{Ca}^{2+}$  is also used as a tracer for mineral dust, which commonly enters the atmosphere via road wear, gritting and dust resuspension due to transport, as well as via gusts of wind (Denier van der Gon et al., 2010). At the Swiss sites, Ca metal was measured as opposed to the soluble ion  $\text{Ca}^{2+}$ , but is still a suitable tracer for mineral dust. Titanium metal is also used as a chemical tracer for mineral dust and thus should possess a similar resuspension mechanism (Charron et al., 2019). A positive correlation with these dust tracers would suggest plant debris is resuspended into the atmosphere via the same established mechanism as mineral dust.

Considering EC first, Table 5 shows typically weak positive correlations between EC and cellulose abundance at sites considered to be urban or traffic-impacted in character, excluding Les Frênes ( $R_s$  0.25 – 0.34,  $p < 0.03$ ). The rural-based sites showed very little correlation ( $R_s$  -0.03 – 0.11,  $p$  0.16 – 0.79), suggesting that any resuspension mechanism of plant debris involving automotive vehicles is only active in more built-up areas. In any case, automotive resuspension of plant debris appears to be relatively weak, even when present at the more urban locations.

In general, cellulose correlations with the two mineral dust chemical tracers were slightly stronger across all sites compared to their respective cellulose-EC correlations. These values were once again higher at more urban locations compared to rural sites, in particular at Basel and Bern, which show  $R_s$  values between 0.37 and 0.45 ( $p < 0.001$ ). The stronger correlations with mineral dust do seem to suggest that ambient cellulose concentrations are somewhat influenced by the resuspension of plant debris in a manner similar to that of mineral dust. Yet, given the lack of significant correlation with EC, it seems that a resuspension mechanism may not include a vehicular input. Other anthropogenic resuspension mechanisms not related to traffic may contribute; paper usage (e.g. newspaper and cardboard production) has been mooted in previous literature (Caseiro, 2008). These still unknown mechanisms could shadow the seasonality of cellulose concentrations in more urban locations. One possible process without anthropogenic input, however, could be via strong gusts of wind that resuspend this



plant material. Agricultural activities can also play a large role in emitting plant matter into the atmosphere. Samaké et al. (2019b) showed maximum cellulose concentrations occurred during harvest (summer) at ANDRA-OPE. This agricultural input from harvested land is also a major emission source of polyols and glucose, which may explain the strong correlations of cellulose with these tracers at the more rural locations (Samaké et al., 2019b). A lot of these processes (seed emission, harvest, mowing, tree cutting, street sweeping and traffic etc.) are highly sporadic and are subject to significant uncertainties, such as particle loads before, during and after rain.

Overall, several conclusions can be drawn for the three potential sources proposed in the literature. Firstly, the direct biogenic source of atmospheric plant debris is by far the most significant, showing moderate to strong Spearman correlations between cellulose and other characteristic biogenic tracers. This is particularly clear in rural sites; the correlation is inconsistent among other site types. In addition, there is no source of atmospheric plant debris that arises from biomass burning across any season or site type, as already suggested by Borlaza et al. (2021a). Lastly, the resuspension of plant material could be another possible input to overall ambient plant debris abundance. This mechanism does not seem to incorporate road traffic in the way suggested by Caseiro (2008), given the lack of correlation between cellulose and EC abundance.

### **3.6 Local vs. regional origin**

Seasonal cellulose variations do not show a similar pattern across all sites, nor one that is consistent across different regions and scales. This trend, or lack thereof, was expressed numerically using correlation coefficients ( $R^2$ ) of monthly concentration averages for the groups of sites that were sampled at the same time. As shown in Table 6, the correlations between sites within the Grenoble metropole (CB, LF and Vif) are low to moderate. This is also the case for the Swiss sites, which span a much larger spatial range compared to the Grenoble-based sites. The lack of a shared temporal variability seems to indicate that the major sources of plant debris are most likely to be local to each site. It may also suggest that several mechanisms impacting ambient cellulose concentrations contribute to different degrees according to the investigated site (Caseiro, 2008; Winiwarter et al., 2009; Borlaza et al., 2021). Moderate correlations between the traffic-impacted location in Bern with the two rural sites of Magadino and Payerne were the highest among the Swiss sites. Regardless, these values are

not indicative of a common source. The Grenoble-based sites of LF and Vif do seem to show a slight exception, producing an  $R^2$  value close to 0.7 ( $p < 0.0001$ ). The three monitoring locations within the Grenoble metropole are within 15 km of one another, so a common source of atmospheric plant debris on local scales of this magnitude remains possible.

Table 6: Correlations ( $R^2$ ) monthly cellulose concentrations between the Swiss sites (top) and between Grenoble-based (bottom) sites (LF, CB and Vif). The colour-coded key (right) gives the corresponding colour of the correlation strength ( $R^2$  values). A strong correlation ( $R^2$  close to 1) is coded red, with no correlation coded blue. Intermediate correlations are coded white. **Note:** CB = Caserne de Bonne, LF = Les Frênes. Grenoble-based sites represented by CB, LF and Vif.

$R^2$									
Bern	0.0092								
Magadino	0.0059	0.4636							1
Payerne	0.016	0.4275	0.2941						0.8
Zurich	0.0124	0.395	0.1814	0.0046					0.6
	Basel	Bern	Magadino	Payerne					0.5
									0.4
									0.2
									0

$R^2$									
CB	0.0056								
VIF	0.6944	0.0172							
	LF	CB							

Site	LF	CB	VIF	Basel	Bern	Magadino	Payerne	Zurich
Classification	Urban Background	Urban centre	Peri-urban	Suburban	Urban-traffic	Rural	Rural	Urban

The  $R^2$  values in Table 6 were compared to correlations between monthly mean concentrations of the so-called polyol fraction (i.e., sum of arabitol, mannitol and sorbitol) for the same set of locations (Samaké et al., 2019a; Borlaza et al., 2021a; Grange et al., 2021). In contrast to cellulose, polyols show common temporal variations, with  $R^2$  correlations ranging from 0.4 – 0.91 and 0.95 – 0.98 ( $p < 0.0001$ ) within the groups of Swiss and Grenoble-based sites, respectively (Table S6 and Table S7). Polyols are used as chemical tracers for fungal spores, a very common class of PBAP, and here provide a near perfect example of a PBAP class displaying homogenized concentration variations over time at a regional scale. This suggests a single common source of polyols that is impacted similarly by external factors across all locations, especially at short range e.g. within the Grenoble area. This was also suggested by Borlaza et al. (2021) during their PMF study, and by Samaké et al. (2019a) as part of their study across all of France. Moreover, Samaké et al. (2020, 2021) evidenced that the presence

of fungi and bacteria in ambient air is mostly related to a limited number of microorganism species only, which vary from one climatic region to the next.

The stark contrast between the two sets of chemical tracers (cellulose vs. polyols) highlights the rather local nature of atmospheric plant debris and its sources. Given that meteorology is relatively consistent on a short to medium scale (< 200 km), it would be expected that plant debris emissions would impact all sites of a given area similarly. However, heterogeneous distribution of the diverse plant species at the city (or regional) scale might induce specific temporal variations in the emissions of plant debris at the local scale. Therefore, the lack of correlation in cellulose datasets may result from site-to-site differences in the dominant sources (flora) or emission processes of ambient plant debris (Caseiro, 2008).

### **3.7 Interannual Comparison – A Combined Approach**

Cellulose concentrations were measured over two separate time periods: 2017-18 and 2020-21 in Grenoble, and over three separate time periods: 2016, 2017 and 2020 at ANDRA-OPE. These multiple datasets (with a similar number of data points) gave us the opportunity to assess the interannual variations of atmospheric plant debris, in the same regions. This provided the possibility to combine the various analyses used in the above sections as part of a more small-scale, holistic investigation.

#### **Grenoble**

Figure 6 presents the seasonal mean cellulose concentrations across the two time periods within the Grenoble metropole (expressed numerically in Table S8, SI). The difference in cellulose concentrations between different sampling years is stark. Both CB and Vif show significant decreases in cellulose concentrations from 2017-18 to 2020-21, with the exception of the spring period. For example, summer and autumn cellulose concentrations decreased by over a factor of 3 between 2017-18 and 2020-21. This is not the case for the urban background site of Les Frênes, where the seasonal concentrations typically increased across all seasons except for spring.

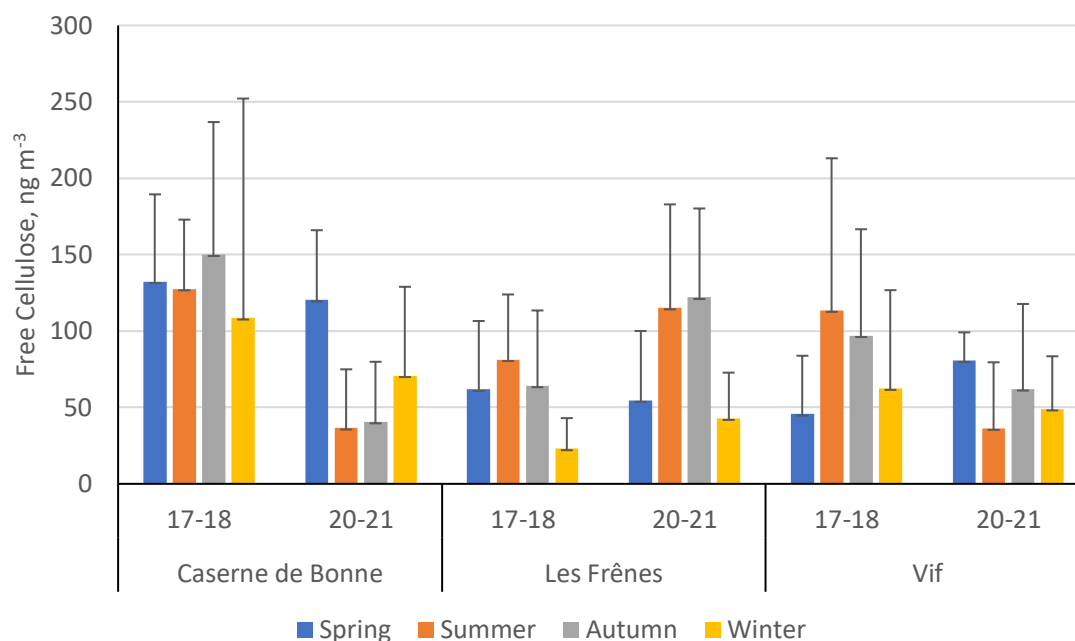


Figure 6: Seasonal mean averages of cellulose concentrations ( $\text{ng m}^{-3}$ ) of the three sites within the Grenoble metropole across the two separate sampling periods: 2017-18 and 2020-21. Black error bars represent one standard deviation of the seasonal means. Only positive error bars are shown to aid clarity. Seasons are defined as: Dec-Feb (winter), Mar-May (spring), Jun-Aug (summer), Sep-Nov (autumn). Site classifications are as follows: Caserne de Bonne – urban; Les Frênes – urban background; Vif – peri-urban.

Temperature data was used as an attempt to elucidate the contrasting concentrations across the two sampling periods (Fig. S4, SI). A warmer and more humid climate brings about greater biological activity (e.g. an increase in pollen production), but can also speed up the decomposition processes involved in generating plant debris (Liu et al., 2006; Martínez et al., 2014; Verma et al., 2018). Temperature data for Grenoble across the two sampling periods was provided by Atmo Auvergne-Rhône-Alpes (Atmo AURA).

Seasonal and monthly average temperatures across the two sampling periods show some differences, but the variation is slight (Fig. S4, SI). It is highly unlikely in this instance that the large variations in the atmospheric cellulose concentrations were caused by ambient temperature changes. This is further supported by the lack of change in seasonal average polyol concentrations for the same sites, shown in Fig. S5, whose concentrations are impacted solely by biogenic factors (Bauer et al., 2008; Zhang et al., 2010; Després et al., 2012). While other climate data were not been available, there is potential for the variability in cellulose source strengths to have been caused by factors that are not purely meteorological. This observed variability may be related to changes in human activities, associated with the COVID-19

lockdown and sanitary restrictions. This would most profoundly affect the pedestrianised urban centre of Caserne de Bonne, with the prolonged closure of shops in the area surrounding the sampling site, together with the decrease of traffic on the nearby avenues.

Interestingly, changes in ambient cellulose concentrations across the two periods are concomitant with changes in the contribution of cellulose-C to OC (Fig. 7, numerical values Table S9). Thus, it is likely that changes in atmospheric cellulose concentrations will have resulted from changes in the source strength of plant debris, and not from a wider-scale reduction in some or all other OC sources.

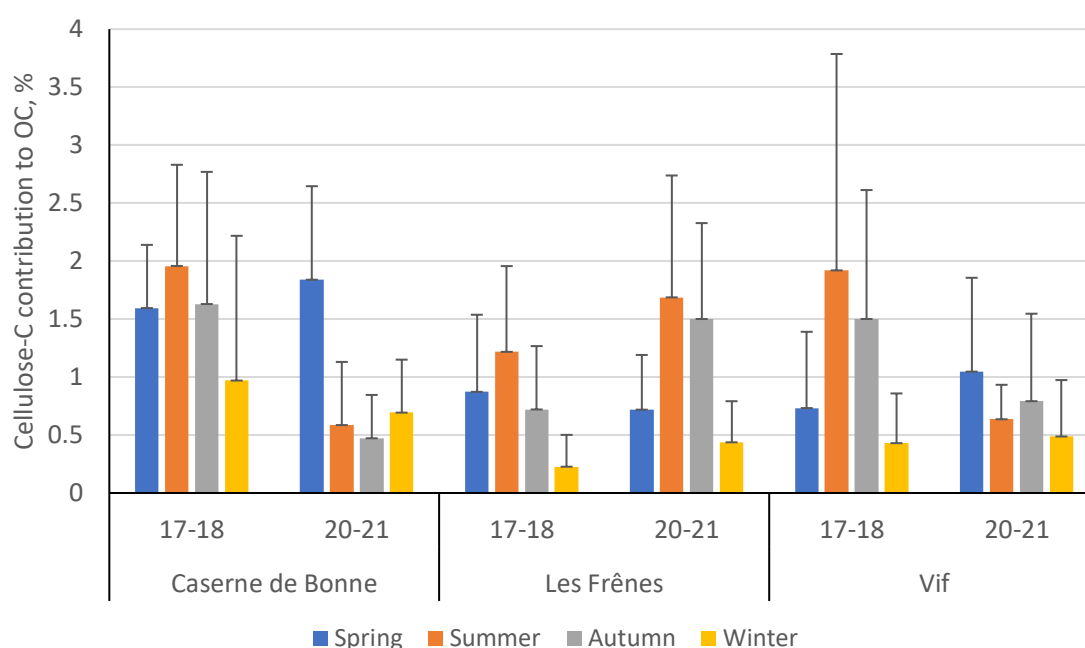


Figure 7: Percentage contribution of cellulose-derived carbon towards overall organic carbon (cellulose-C to OC) across the three sites within the Grenoble metropole during the two separate sampling periods: 2017-18 and 2020-21. Black error bars represent one standard deviation of the seasonal means. Only positive error bars are shown to aid clarity. Seasons are defined as: Dec-Feb (winter), Mar-May (spring), Jun-Aug (summer), Sep-Nov (autumn).

Site classifications are as follows: Caserne de Bonne – urban; Les Frênes – urban background; Vif – peri-urban.

Given that these large interannual variations seemed to be predominantly limited to cellulose and not the remaining sources of OC, it was necessary to evaluate the potential sources once more. Following section 3.5, cellulose-tracer correlations were again produced using the same characteristic source tracers for the two periods, to see if changes in cellulose concentrations were consistent with variations in tracer correlations. These correlation coefficients can be seen in Table 7 (Table S10 for full table). From the two sets of correlations, it is evident that the

sources of plant debris are only consistent between campaigns at Les Frênes. Reasonable correlations with characteristic biogenic chemical tracers (polyols and glucose) remain consistent, whilst a moderate anti-correlation is still seen between cellulose and levoglucosan. No correlations with EC were seen throughout the two campaigns.

*Table 7: Spearman correlations ( $R_s$ ) between cellulose and characteristic chemical tracers at the Grenoble-based sites, across the two separate sampling periods: 2017-18; 2020-21. A red cell indicates a positive correlation between cellulose and the selected chemical tracer, whilst a blue cell indicates a negative correlation. A colour-coded key of corresponding  $R_s$  values is to the right of the table.*

*Site classifications are as follows: Caserne de Bonne (CB) – urban; Les Frênes (LF) – urban background; Vif – peri-urban. **Note: polyols = sum of arabitol, mannitol and sorbitol.***

$R_s$	Grenoble 2017 - 2018			Grenoble 2020 - 2021			
	CB	LF	Vif	CB	LF	Vif	
Polyols	0.46	0.63	0.59	-0.09	0.68	0.22	1.00
Glucose	0.47	0.62	0.66	-0.08	0.56	0.24	0.66
Levoglucosan	-0.07	-0.48	-0.21	0.25	-0.38	0.10	0.33
EC	0.15	-0.11	-0.07	0.18	0.01	0.16	0.00
Ca <sup>2+</sup>	0.14	0.22	0.00	0.31	0.32	0.32	-0.33
							-0.66
							-1.00

By contrast, tracer correlations across both CB and Vif vary significantly between the two campaigns.  $R_s$  values of cellulose versus glucose or polyol concentrations decrease significantly during the 20/21 campaign. A weak positive correlation becomes apparent between cellulose and Ca<sup>2+</sup> concentrations during the 20/21 campaign that was absent during the previous series. This is particularly visible at Vif, but it is also a consistent trend across all three sites. These findings suggest potentially two possible hypotheses. Firstly, the contribution of plant debris arising from biogenic sources has been much weaker during the second campaign at CB and Vif, compared to three years earlier, thus showing little to no correlation with characteristic biogenic tracers. This may be the reason for the weakened seasonality at both CB and Vif. Secondly, the increased correlation with Ca<sup>2+</sup> during 20/21 implies a better correlation between plant debris and mineral dust abundance. This in turn could suggest a slight increase in the strength of plant matter resuspension during the second campaign, compared to 2018-19.



## ANDRA-OPE

Figure 8 shows the seasonal mean average free cellulose concentrations ( $\text{ng m}^{-3}$ ) for three separate sampling campaigns (2016, 2017 and 2020) at ANDRA-OPE (numerical values in Table S11, SI). During the 2017 monitoring campaign, an extended period of sampling was completed with samples being taken on average 5 times per week during summer. For this interannual analysis, it was important to bring the number of data points in line with the datasets from 2016 and 2020. Samples were removed from the 2017 dataset until the same sampling frequency was obtained across all the periods (1 sample taken every sixth day). As can be seen in Fig. 8, cellulose concentrations dropped significantly between 2016/2017 and 2020, with the exception of the winter period. This is in a manner very similar to the variations seen at the CB and Vif sampling sites from within the Grenoble metropole. The data for the winter period in

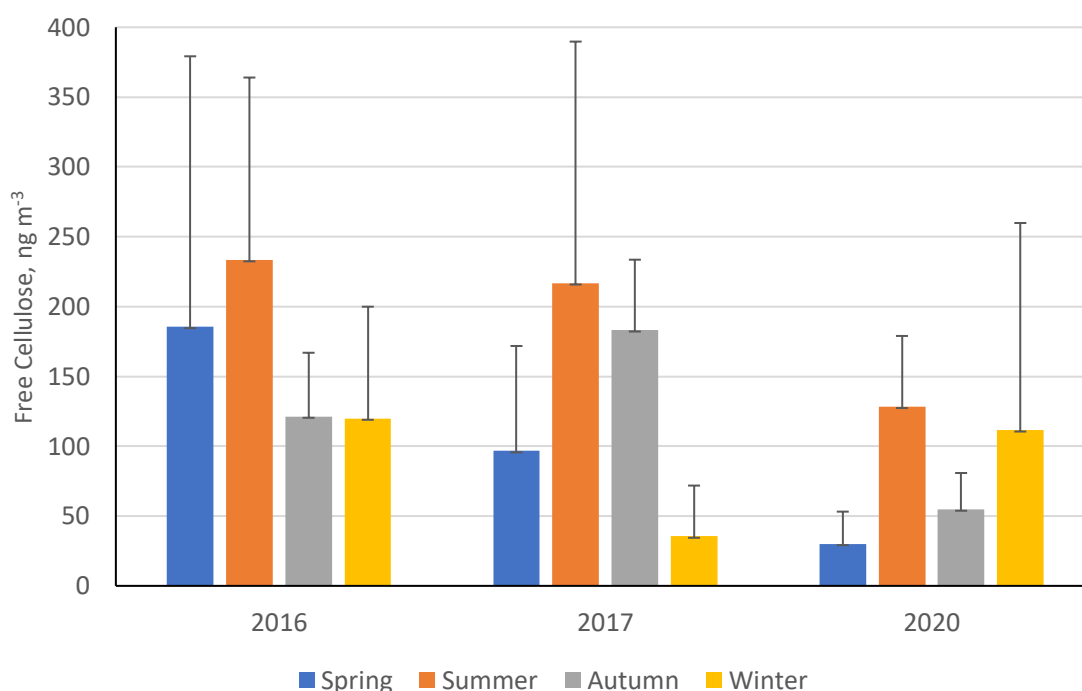


Figure 8: Seasonal mean averages of cellulose concentrations ( $\text{ng m}^{-3}$ ) at ANDRA-OPE (rural site) during the three separate sampling periods: 2016, 2017 and 2020. Black error bars represent one standard deviation of the seasonal means. Only positive error bars are shown to aid clarity. Seasons are defined as: Dec-Feb (winter), Mar-May (spring), Jun-Aug (summer), Sep-Nov (autumn).

2020 comes predominantly from before the COVID-19 pandemic, so it is possible for the significant reduction in anthropogenic activities being a major factor in the reduction of atmospheric cellulose concentrations. However, it should be mentioned that agricultural

activities (fertilisation, harvest, ploughing, etc...) were not affected by the COVID-19 associated restrictions.

Further, we once again see a noticeable reduction in the contribution of cellulose-C to OC (%) during the 2020 sampling period, compared to the two previous campaigns, especially during summer and autumn (Fig. 9, numerical values Table S12, SI). This suggests that the source of atmospheric plant debris became significantly weaker during 2020, when placed in the context of overall OC atmospheric emission. Unlike the Grenoble metropole dataset, at ANDRA-OPE the seasonal variations of cellulose concentrations and the respective contributions of cellulose-C to overall OC are different. This may suggest that other emission sources of OC have varied at ANDRA-OPE, compared to the more consistent OC emission within Grenoble across its sampling periods.

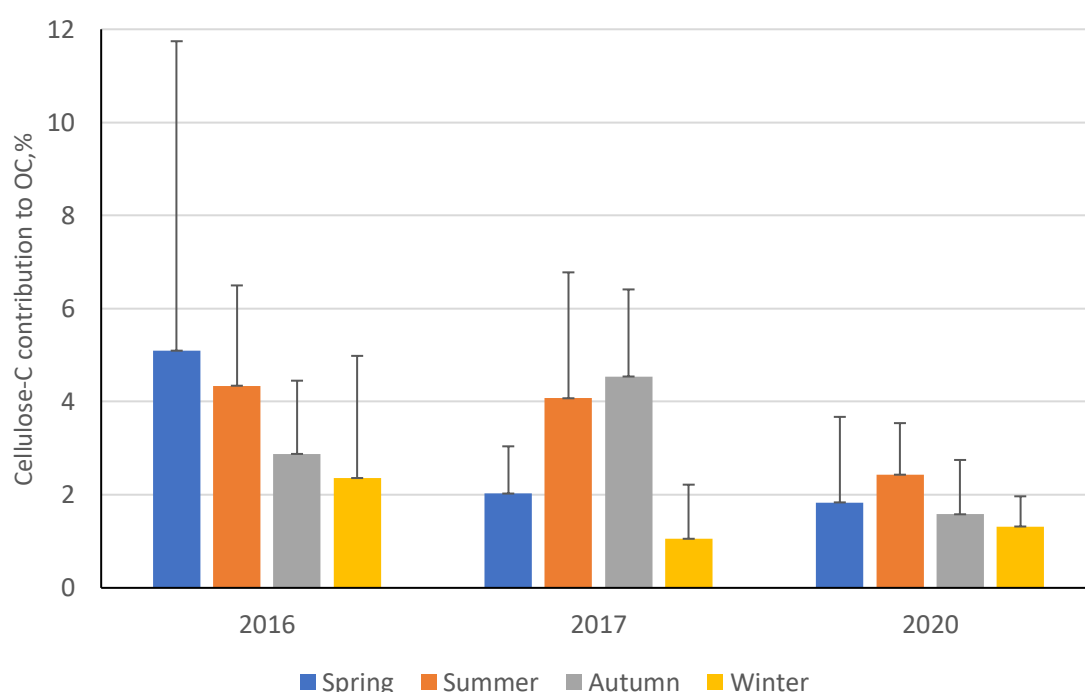


Figure 9: Percentage contribution of cellulose-carbon towards overall organic carbon (cellulose-C to OC) at ANDRA-OPE during the three separate sampling periods: 2016, 2017 and 2020. Black error bars represent one standard deviation of the seasonal means. Only positive error bars are shown to aid clarity. Seasons are defined as: Dec-Feb (winter), Mar-May (spring), Jun-Aug (summer), Sep-Nov (autumn).

Following these significant interannual variations within cellulose concentrations and cellulose-C to OC, correlations of cellulose with source-specific tracers were completed to see how the source of atmospheric plant debris has changes between the three sampling periods (Table 8, p values in Table S13, SI). The three sampling periods at ANDRA-OPE exhibit significant variations in their cellulose-tracer correlations. Notably, the correlations of cellulose with biogenic tracers (polyols and glucose) remain generally moderate throughout,

and in fact are weakest during the 2016 campaign. This suggests that, at the rural site of ANDRA-OPE, the significant reduction in atmospheric cellulose concentrations during 2020 is consistent with that of the changes within other biogenic chemical tracers. Further, during the 2020 campaign, a relatively strong correlation is seen between cellulose and  $\text{Ca}^{2+}$ , a mineral dust tracer, that is absent during the previous two campaigns. This potentially implies a significant contribution to cellulose concentrations from an anthropogenic source, or reflects a correlation to wind speed. An anthropogenic source would be unlikely however, given the rural nature of this sampling site and its lack of proximity to anthropogenic inputs, outside of agriculture.

*Table 8: Spearman correlations ( $R_s$ ) between cellulose and characteristic chemical tracers at ANDRA-OPE, across the three separate sampling periods: 2016, 2017 and 2020. A red cell indicates a positive correlation between cellulose and the selected chemical tracer, whilst a blue cell indicates a negative correlation. A colour-coded key of corresponding  $R_s$  values is to the right of the table. **Note: polyols = sum of arabitol, mannitol and sorbitol.***

$R_s$	ANDRA-OPE			
	2016	2017	2020	
Polyols	0.44	0.52	0.63	1.00
Glucose	0.21	0.57	0.41	0.66
Levoglucosan	-0.31	-0.30	-0.68	0.33
EC	-0.12	0.03	0.08	0.00
$\text{Ca}^{2+}$	0.23	0.11	0.62	-0.33
				-0.66
				-1.00

Overall, these results at ANDRA-OPE and within the Grenoble conurbation indicate for the first time a large interannual variability in the sources and drivers of atmospheric cellulose, and highlight our emerging knowledge of these processes.

## 4. Conclusions

Previous work has acknowledged the potential contribution of atmospheric cellulose to  $\text{PM}_{10}$  and atmospheric OC (Yttri et al., 2011b; Bozzetti et al., 2016; Borlaza et al., 2021). Yet, long-term studies using cellulose as a chemical tracer for atmospheric plant debris are still rare, and typically cover only few ambient conditions (Sánchez-Ochoa et al., 2007; Caseiro, 2008; Yttri et al., 2011a; Yttri et al., 2011b; Alves, 2017). Thus, an investigation of ambient cellulose concentrations, across a wide range of locations and site types, using a sensitive HPLC-PAD analysis and an improved hydrolysis method was undertaken. To date, with more than 1500

822 samples analysed in the exact same way, this is one of the most in-depth study of atmospheric  
823 cellulose, its seasonality, spatiotemporal variability and its sources.

824  
825 Annual mean free cellulose concentrations were found to range between  $29 \pm 38 \text{ ng m}^{-3}$  at  
826 Basel to  $284 \pm 225 \text{ ng m}^{-3}$  at Payerne (suburban and rural sites, respectively). All rural sites and  
827 half of the urban sites showed cellulose concentrations that were highest during summer and  
828 autumn, coinciding with typically higher seasonal temperatures. This seasonality differs from  
829 the spring-summer maximum illustrated by Sánchez-Ochoa et al. (2007). The remaining urban  
830 sites deviated significantly from this pattern, showing no evidence of seasonal cellulose  
831 variations. This suggests that different sources or processes may shadow the cellulose  
832 seasonality in some urban areas. Cellulose concentrations generally correlated poorly between  
833 sites, which implies a source of atmospheric plant debris that is highly localised.

834  
835 For the first time, correlations of cellulose with chemical tracers, that are characteristic of  
836 specific emissions sources, were completed to best apportion the origins of atmospheric plant  
837 debris. It was shown that plant debris arises predominantly via direct biogenic emissions,  
838 particularly at rural locations. Further, the sites showing the strongest correlations with  
839 biogenic tracers were the same sites that exhibited the general summer-autumn cellulose  
840 maxima. A potential secondary influence towards ambient cellulose concentrations comes via  
841 resuspension of previously settled plant matter, comparable to that of mineral dust. The  
842 mechanism associated with this source is unknown but is unlikely to possess a traffic signature  
843 at the sites investigated, given the poor cellulose correlations with EC, a known tracer for  
844 anthropogenic combustion mainly related to traffic in urban areas. This may be the factor that  
845 masks seasonality at some urban sites. At rural locations, agricultural activities can be a  
846 significant source of cellulose into the atmosphere during harvest, as demonstrated by Samaké  
847 et al. (2019b). Lastly, biomass burning is not a source of atmospheric cellulose for the sites  
848 investigated here.

849  
850 The annual contribution of free cellulose-derived carbon to total organic carbon ranged  
851 between 0.7 and 5.9 % for the measured locations, with rural sites typically showing higher  
852 contributions. It should be noted that the percentage contribution of total cellulose-derived  
853 carbon to OC would be greater than the above values. While the annual mean contributions to  
854 OC seem moderate, this percentage can greatly increase during episodic cellulose  
855 concentration spikes. The maximum percentage contributions seen of cellulose-C to OC at

Payerne and ANDRA-OPE were 19.7 and 18.3% respectively, which are consistent with other background sites results found in the literature. These significant episodic contributions show that cellulose and plant debris can play a significant role in the atmospheric composition.

The interannual variations of the cellulose concentrations at the same locations within the Grenoble metropole were then assessed. Interestingly, the cellulose concentrations and the contribution (%) of cellulose-C to OC showed significant fluctuations across the two periods considered. The correlations of cellulose with other chemical tracers also vary significantly. Reasons behind these dramatic fluctuations are not fully understood and this highlights our limited knowledge of these atmospheric processes. Reduced human activities due to the COVID-19 pandemic may be a factor. Further interannual studies must be undertaken to see if these variations are a common occurrence, or unique to this dataset.

Given the local-scale source of atmospheric plant debris, more monitoring campaigns similar to the one in the Grenoble metropole should be performed. An increase in sampling site numbers, with varying micro-climatic and PM emission source characteristics, within a given area should lead to a more concrete understanding of the spatial variability of plant debris. It would open the road for the inclusion of cellulose into chemical transport models, in order to better represent this component of the organic matter in PM, particularly important in rural areas.

**Data availability:** All relevant data for this paper are archived at the IGE (Institut des Géosciences de l'Environnement), and availability can be discussed with the corresponding authors (Jean-Luc Jaffrezo).

**Acknowledgements:** The authors acknowledge the work of the many engineers in the lab at IGE for the analyses (C. Voiron, R. Elazzouzi, B. Morisset, C. Le Bigaignon, J. Chazelle, A. Vella, G. Fonkoh) as well as the dedicated efforts of many people at the sampling sites for collecting the samples. A. M. Brighty would also like to thank S. Weber for his help and guidance throughout the project. Samples from the 3 Grenoble sites were collected and analysed within the program QAMECS (ADEME 1662C0029), coupled with funding from the CARA program from LCSQA for the “Les Frênes” site.

The authors would like to thank all 3 referees for insightful comments that helped improving the paper. Particularly, Pr Hans Puxbaum provided a long, precise, and detail text with account of the historical aspects of past research on cellulose measurements in atmospheric PM, which is extremely interesting and complete. His comments are now partially reflected in our paper, but the original texts (RC1 and RC4) should be referred to, in order to give him full credit on this point.

896 **Author contributions:** AMB performed all cellulose analyses, processed the data and wrote  
 897 up the manuscript. JLJ was the supervisor for the Masters of AMB. He directed all the  
 898 personnel who performed the analysis at IGE and designed the study. VJ designed the protocol  
 899 for cellulose analyses. JLJ and GU were the coordinators of the atmospheric part of the  
 900 Mobil’Air program in Grenoble; LJB was the curator of the atmospheric Mobil’Air data. SB  
 901 is the coordinator of the ANDRA-OPE site and atmospheric program, and provided the samples  
 902 from this site. CH is the head of the NABEL network in Switzerland, provided all samples  
 903 from this country and directed the program for this yearly sampling; SKG was the curator of  
 904 the swiss data. OF is responsible for the CARA program from the LCSQA in France, and  
 905 provided partial funding for sample analysis at LF site. CT was responsible for the sampling  
 906 by Atmo-AURA at the 3 sites in the Grenoble area. All authors reviewed and commented on  
 907 the manuscript.

908 **Competing interests:** The authors declare that they have no conflict of interest.

## 909 **References**

- 910 Alfarra, M. R., Prevot, A. S. H., Szidat, S., Sandradewi, J., Weimer, S., Lanz, V. A., Schreiber,  
 911 D., Mohr, M., and Baltensperger, U.: Identification of the mass spectral signature of organic  
 912 aerosols from wood burning emissions, *Environ. Sci. Technol.*, 41, 5770-5777, 2007.
- 913 Alleman, L. Y., Lamaison, L., Perdrix, E., Robache, A. and Galloo, J.-C.: PM10 metal  
 914 concentrations and source identification using positive matrix factorization and wind sectoring  
 915 in a French industrial zone, *Atmospheric Research*, 96(4), 612–625,  
 916 <https://doi.org/10.1016/j.atmosres.2010.02.008>, 2010.
- 917  
 918 Alves, C. A.: A short review on atmospheric cellulose, *Air Qual. Atmos. Health*, 10, 669–678,  
 919 2017.
- 920 Atmo AURA: <https://www.atmo-auvergnerhonealpes.fr/>, last access: 12 April 2021.
- 921 Aymoz, G., Jaffrezo, J. L., Chapuis, D., Cozic, J., and Maenhaut, W.: Seasonal variation of PM  
 922 10 main constituents in two valleys of the French Alps. I: EC/OC fractions, *Atmos. Chem.*  
 923 *Phys.*, 7(3), 661–675, 2007.
- 924 Bauer, H., Claeys, M., Vermeylen, R., Schueller, E., Weinke, G., Berger, A., and Puxbaum,  
 925 H.: Arabitol and mannitol as tracers for the quantification of airborne fungal spores, *Atmos.*  
 926 *Environ.*, 42(3), 588–593, 2008a.
- 927 Birch, M. E. and Cary, R. A.: Elemental carbon-based method for monitoring occupational  
 928 exposures to particulate diesel exhaust, *Aerosol Sci. Technol.*, 25(3), 221–241, 1996.
- 929 Borlaza, L. J. S., Weber, S., Uzu, G., Jacob, V., Cañete, T., Micallef, S., Trébuchon, C., Slama,  
 930 R., Favez, O., Jaffrezo, J., L.: Disparities in particulate matter (PM10) origins and oxidative  
 931 potential at a city-scale (Grenoble, France) - Part I: Source apportionment at three neighbouring  
 932 sites, *Atmos. Chem. Phys.*, 21(7), 5415–5437, 2021a.

- 933 Borlaza, L. J. S., Weber, S., Jaffrezo, J. L., Houdier, S., Slama, R., Rieux, C., Albinet, A.,  
 934 Micallet, S., Trébuchon, C., and Uzu, G.: Disparities in PM<sub>10</sub> origins and oxidative potential at  
 935 a city-scale (Grenoble, France) - Part II: Sources of PM<sub>10</sub> oxidative potential using multiple  
 936 linear regression analysis and the predictive applicability of multilayer perceptron neural  
 937 network analysis, *Atmos. Chem. Phys.*, 21(12), 9719–9739, [https://doi.org/10.5194/acp-21-](https://doi.org/10.5194/acp-21-9719-2021)  
 938 9719-2021, 2021b.
- 939 Borlaza, L. J. S., Weber, S., Marsal, A., Uzu, G., Jacob, V., Besombes, J. L., Conil, S., and  
 940 Jaffrezo, J. L.: Long-term trends of PM<sub>10</sub> sources and oxidative potential in a rural site in  
 941 France. Submitted to *Atmos. Chem. Phys. Disc.*, on 18/10/2021, 2021c.
- 942 Boucher, O., Randall, D., Artaxo, P., Bretherton, C., Feingold, G., Forster, P., Kerminen, V.-  
 943 M., Kondo, Y., Liao, H., and Lohmann, U.: Clouds and aerosols, in *Climate change 2013: the*  
 944 *physical science basis. Contribution of Working Group I to the Fifth Assessment Report of the*  
 945 *Intergovernmental Panel on Climate Change*, pp. 571– 657, Cambridge University Press.,  
 946 2013.
- 947 Bozzetti, C., Daellenbach, K. R., Heuglin, C., Fermo, P., Sciare, J., Kasper-Giebl, A., Mazar,  
 948 Y., Abbaszade, G., El Kazzi, M., Gonzalez, R., Shuster-Meiseles, T., Flasch, M., Wolf, R.,  
 949 Kreplová, A., Canonaco, F., Schnelle-Kreis, J., Slowik, J. G., Zimmermann, R., Rudich, Y.,  
 950 Baltensperger, U., El Haddad, I., and Prévôt, A. S. H.: Size-Resolved Identification,  
 951 Characterisation, and Quantification of Primary Biological Organic Aerosol at a European  
 952 Rural Site, *Environ. Sci. Technol.*, 50, 3425 – 3434, 2016.
- 953 Caseiro, A. F. F.: *Composição Química do Aerossol Europeu.*, PhD Thesis, Universidade de  
 954 Aveiro, Aveiro. [online] Available from: <https://core.ac.uk/download/pdf/15560924.pdf>  
 955 (Accessed 27 October 2020), 2008.
- 956 Cavalli, F., Viana, M., Yttri, K. E., Genberg, J., and Putaud, J.-P.: Toward a standardised  
 957 thermal-optical protocol for measuring atmospheric organic and elemental carbon: the  
 958 EUSAAR protocol, *Atmos. Meas. Tech.*, 3(1), 79–89, 2010.
- 959 Charron, A., Polo-Rehn, L., Bescombes, J. L., Golly, B., Buisson, C., Chanut, H., Marchand,  
 960 N., Guillaud, G., and Jaffrezo, J. L.: Identification and quantification of particulate tracers of  
 961 exhaust and non-exhaust vehicle emissions for source apportionment studies, *Atmos. Chem.*  
 962 *Phys.*, 19(7), 5187–5207, <https://doi.org/10.5194/acp-19-5187-2019>, 2019.
- 963 Chevrier, F.: *Chauffage au bois et qualité de l’air en Vallée de l’Arve : définition d’un système*  
 964 *de surveillance et impact d’une politique de rénovation du parc des appareils anciens.*, PhD  
 965 Thesis, Université Grenoble Alpes, Grenoble. [online] Available from: [https://tel.archives-](https://tel.archives-ouvertes.fr/tel-01527559)  
 966 [ouvertes.fr/tel-01527559](https://tel.archives-ouvertes.fr/tel-01527559) (Accessed 5 January 2021), 2016.
- 967 Denier van der Gon, H., Jozwicka, M., Hendriks, E., Gondwe, M., and Schaap, M.: Mineral  
 968 Dust as a component of Particulate Matters, BOP Reports, The Netherlands, 2010.
- 969 Després, V. R., Alex Huffman, J., Burrows, S. M., Hoose, C., Safatov, A. S., Buryak, G.,  
 970 Fröhlich-Nowoisky, J., Elbert, W., Andreae, M. O., Pöschl, U., and Jaenicke, R.: Primary

971 biological aerosol particles in the atmosphere: a review, *Tellus B: Chemical and Physical*  
972 *Meteorology*, 64, 15598, 2012.

973 Franke, V., Zieger, P., Wideqvist, U., Acosta Navarro, J. C., Leck, C., Tunved, P., Rosati, B.,  
974 Gysel, M., Salter, M. E., and Ström, J.: Chemical composition and source analysis of  
975 carbonaceous aerosol particles at a mountaintop site in central Sweden, *Tellus B Chem. Phys.*  
976 *Meteorol.*, 69(1), 1353387, <https://doi.org/10.1080/16000889.2017.1353387>, 2017.  
f

977 Gelencsér, A., May, B., Simpson, D., Sánchez-Ochoa, A., Kasper-Giebl, A., Puxbaum, H.,  
978 Caseiro, A., Pio, C. and Legrand, M.: Source apportionment of PM<sub>2.5</sub> organic aerosol over  
979 Europe: Primary/secondary, natural/anthropogenic, and fossil/biogenic origin, *J. Geophys.*  
980 *Res.*, 112(D23), D23S04, <https://doi.org/10.1029/2006JD008094>, 2007.

981 Gelencsér, A.: *Carbonaceous Aerosol*, 1<sup>st</sup> edn, Springer, The Netherlands, 350 pages, 2004.

982 Giannoni, M., Martellini, T., Del Bubba, M., Gambaro, A., Zangrando, R., Chiari, M., Lepri,  
983 L., and Cincinelli, A.: The use of levoglucosan for tracing biomass burning in PM<sub>2.5</sub> samples in  
984 Tuscany (Italy), *Environmental Pollution*, 167, 7–15, 2012.

985 Golly, B., Waked, A., Weber, S., Samaké, A., Jacob, V., Conil, S., Rangonio, J., Chrétien, E.,  
986 Vagnot, M. P., Robic, P. Y., Besombes, J. L., and Jaffrezo, J. L.: Organic Markers And OC  
987 Source Apportionment For Seasonal Variations Of PM<sub>2.5</sub> At 5 Rural Sites In France, *Atmos.*  
988 *Environ.*, 198, 142-157, <https://doi.org/10.1016/J.Atmosenv.2018.10.027>, 2019.

989 Gould, M. J.: Alkaline peroxide delignification of agricultural residues to enhance enzymatic  
990 saccharification, *Biotechnol. Bioengng*, 26, 46–52, 1984.

991 Graham, B., Guyon, P., Taylor, P. E., Artaxo, P., Maenhaut, W., Glovsky, M. M., Flagan, R.  
992 C., and Andreae, M. O.: Organic compounds present in the natural Amazonian aerosol:  
993 Characterization by gas chromatography-mass spectrometry: Organic compounds in  
994 Amazonian aerosols., *J. Geophys. Res. Atmospheres*, 108(D24), 4766, 2003.

995 Grange, S. K., Fischer, A., Zellweger, C., Alastuey, A., Querol, X., Jaffrezo, J. L., Uzu, G.,  
996 and Hueglin, C.: Switzerland's PM<sub>10</sub> and PM<sub>2.5</sub> environmental increments show the  
997 importance of non-exhaust emissions, *Atmos. Environ.*, submitted (on 22/06/21).

998 Hansen, A.D., Rosen, H. and Novakov, T.: The Aethalometer: An Instrument for the Real Time  
999 Measurement of Optical Absorption by Particles, *Sci. Tot. Enviro.*, 36, 191–196,  
1000 [https://doi.org/10.1016/0048-9697\(84\)90265-1](https://doi.org/10.1016/0048-9697(84)90265-1), 1984.

1001 Jaenicke, R.: Abundance of cellular material and proteins in the atmosphere, *Science*,  
1002 308(5718), 73–73, <https://doi.org/10.1126/science.1106335>, 2005.

1003 Jaffrezo, J. L., Calas, N., and Bouchet, M.: Carboxylic acids measurements with ionic  
1004 chromatography, *Atmos. Environ.*, 32(14), 2705–2708, 1998.

1005 Jia, Y., Bhat, S., and Fraser, M. P.: Characterization of saccharides and other organic  
1006 compounds in fine particles and the use of saccharides to track primary biologically derived  
1007 carbon sources, *Atmos. Environ.*, 44(5), 724–732, 2010a.



1008 Karagulian, F., Belis, C. A., Dora, C. F. C., Prüss-Ustün, A. M., Bonjour, S., Adair-Rohani,  
1009 and H., Amann, M.: Contributions to cities' ambient particulate matter (PM): A systematic  
1010 review of local source contributions at global level, *Atmos. Environ.*, 120, 475–483, 2015.

1011 Klimont, Z., Kupiainen, K., Heyes, C., Purohit, P., Cofala, J., Rafaj, P., Borken-Kleefeld, J.,  
1012 and Schöpp, W.: Global anthropogenic emissions of particulate matter including black carbon,  
1013 *Atmos. Chem. Phys.*, 17, 8681–8723, 2017.

1014 Kunit, M., and Puxbaum, H.: Enzymatic determination of the cellulose content of atmospheric  
1015 aerosols, *Atmos. Environ.*, 30, 1233–1236, 1996.

1016 Liang, L., Engling, G., Du, Z., Cheng, Y., Duan, F., Liu, X., and He, K.: Seasonal variations  
1017 and source estimation of saccharides in atmospheric particulate matter in Beijing, China,  
1018 *Chemosphere*, 150, 365–377, 2016.

1019 Liu, C., Berg, B., Kutsch, W., Westman, C. J., Ilvesniemi, H., Shen, X., Shen, G., and Chen,  
1020 X.: Leaf litter nitrogen concentration as related to climatic factors in Eurasian forests, *Global  
1021 Ecology and Biogeography*, 15, 438–444, 2006.

1022 Madsen, D., Azeem, H. A., Sandahl, M., van Hees, P., and Husted, B.: Levoglucosan as a  
1023 Tracer for Smouldering Fire, *Fire Technology*, 54, 1871–1885, 2018.

1024 Martin, S. T., Andreae, O. M., Artaxo, P., Baumgardner, D., Chen, Q., Goldenstein, A. H.,  
1025 Guenther, A., Heald, C. L., Mayol-Bracero, O. L., McMurry, P. H., Pauliquevis, T., Pöschl,  
1026 U., Prather, K. A., Roberts, G. C., Saleska, S. R., Silva Dias, M. A., Spracklen, D. V.,  
1027 Swietlicki, E., and Trebs, I.: Sources and properties of Amazonian aerosol particles, *Rev.  
1028 Geophys.*, 48(2), <https://doi.org/10.1029/2008RG000280>, 2010.

1029 Martínez, A., Larrañaga, A., Pérez, J., Descals, E., and Pozo, J.: Temperature affects leaf litter  
1030 decomposition in low-order forest streams: field and microcosm approaches, *FEMS Microb.  
1031 Ecol.*, 87, 257–267, 2014.

1032 Medeiros, P. M., Conte, M. H., Weber, J. C., and Simoneit, B. R. T.: Sugars as source indicators  
1033 of biogenic organic carbon in aerosols collected above the Howland Experimental Forest,  
1034 Maine, *Atmos. Environ.*, 40(9), 1694–1705, 2006.

1035 Michoud, V., Hallemans, E., Chiappini, L., Leoz-Garziandia, E., Colomb, A., Dusanter, S.,  
1036 Fronval, I., Gheusi, F., Jaffrezo, J. L., Léonardis, T., Locoge, N., Marchand, N., Sauvage, S.,  
1037 Sciare, J., and Doussin, J. F.: Molecular characterization of gaseous and particulate oxygenated  
1038 compounds at a remote site in Cape Corsica in the western Mediterranean basin, *Atmos. Chem.  
1039 Phys.*, 21(10), 8067–8088, <https://doi.org/10.5194/acp-21-8067-2021>, 2021.

1040 Mobil'Air QAMECS Program: [https://mobilair.univ-grenoble-alpes.fr/mobilair/projets-](https://mobilair.univ-grenoble-alpes.fr/mobilair/projets-associes/projets-associes-743738.htm?RH=2206232030103086)  
1041 [associes/projets-associes-743738.htm?RH=2206232030103086](https://mobilair.univ-grenoble-alpes.fr/mobilair/projets-associes/projets-associes-743738.htm?RH=2206232030103086), last access: 13 April 2021.

1042 Nozière, B., Kalberer, M., Claeys, M., Allan, J., D'Anna, B., Decesari, S., Finessi, E., Glasius,  
1043 M., Grgić, I., Hamilton, J. F., Hoffmann, T., Iinuma, Y., Jaoui, M., Kahnt, A., Kampf, C. J.,  
1044 Kourtchev, I., Maenhaut, W., Marsden, N., Saarikoski, S., Schnelle-Kreis, J., Surratt, J. D.,  
1045 Szidat, S., Szmigielski, R., and Wisthaler, A.: The molecular identification of organic

1046 compounds in the atmosphere: state of the art and challenges, *Chem. Rev.*, 115(10), 3919–  
 1047 3983, <https://doi.org/10.1021/cr5003485>, 2015.

1048 OPE-ANDRA Atmospheric Station: <http://ope.andra.fr/index.php?lang=fr>, last access: 6  
 1049 January 2021.

1050 Peccia, J., Hospodsky, D., and Bibby, K.: New Directions : A revolution in DNA sequencing  
 1051 now allows for the meaningful integration of biology with aerosol science, *Atmos. Environ.*,  
 1052 45, 1896–1897, 2011.

1053 Penner, J. E., Andreae, M., Annegarn, H., Barrie, L., Feichter, J., Hegg, D., Jayaraman, A.,  
 1054 Leaitch, R., Murphy, D., Nganga, J., and Pitari, G.: *Aerosols, their Direct and Indirect Effects*,  
 1055 *Climate Change 2001: The Scientific Basis.*, Cambridge University Press, Cambridge, 2001.

1056 Pöschl, U., Martin, S. T., Sinha, B., Chen, Q., Gunthe, S. S., Huffman, J. A., Borrmann, S.,  
 1057 Farmer, D. K., Garland, R. M., Helas, G., Jimenez, J. L., King, S. M., Manzi, A., Mikhailov,  
 1058 E., Pauliquevis, T., Petters, M. D., Prenni, A. J., Roldin, P., Rose, D., Schneider, J., Su, H.,  
 1059 Zorn, S. R., Artaxo, P., and Andreae, M. O.: Rainforest Aerosols as Biogenic Nuclei of Clouds  
 1060 and Precipitation in the Amazon, *Science*, 329 (5998), 1513–1516, 2010.

1061 Pöschl, U.: Atmospheric Aerosols: Composition, Transformation, Climate and Health Effects,  
 1062 *Angew. Chem. Int. Ed.*, 44(46), 7520 – 7540, 2005.

1063 Putaud, J.-P., Raes, F., Van Dingenen, R., Brüggemann, E., Facchini, M.-C., Decesari, S.,  
 1064 Fuzzi, S., Gehrig, R., Hüglin, C., Laj, P., Lorbeer, G., Maenhaut, W., Mihalopoulos, N., Müller,  
 1065 K., Querol, X., Rodriguez, S., Schneider, J., Spindler, G., Brink, H. ten, Tørseth, K., and  
 1066 Wiedensohler, A.: A European aerosol phenomenology 2: chemical characteristics of  
 1067 particulate matter at kerbside, urban, rural and background sites in Europe, *Atmos. Environ.*,  
 1068 38(16), 2579–2595, 2004a.

1069 Putaud, J.-P., Van Dingenen, R., Alastuey, A., Bauer, H., Birmili, W., Cyrys, J., Flentje, H.,  
 1070 Fuzzi, S., Gehrig, R., Hansson, H. C., Harrison, R. M., Herrmann, H., Hitzenberger, R., Hüglin,  
 1071 C., Jones, A. M., Kasper-Giebl, A., Kiss, G., Kousa, A., Kuhlbusch, T. A. J., Löschau, G.,  
 1072 Maenhaut, W., Molnar, A., Moreno, T., Pekkanen, J., Perrino, C., Pitz, M., Puxbaum, H.,  
 1073 Querol, X., Rodriguez, S., Salma, I., Schwarz, J., Smolik, J., Schneider, J., Spindler, G., ten  
 1074 Brink, H., Tursic, J., Viana, M., Wiedensohler, A. and Raes, F.: A European aerosol  
 1075 phenomenology – 3: Physical and chemical characteristics of particulate matter from 60 rural,  
 1076 urban, and kerbside sites across Europe, *Atmos. Environ.*, 44(10), 1308–1320,  
 1077 <https://doi.org/10.1016/j.atmosenv.2009.12.011>, 2010.

1078 Puxbaum, H., and Tenze-Kunit, M.: Size distribution and seasonal variation of atmospheric  
 1079 cellulose, *Atmos. Environ.*, 37(26), 3693–3699, 2003.

1080 Rogge, W. F., Mazurek, M. A., Hildemann, L. M., Cass, G. R., and Simoneit, B. R. T.:  
 1081 Quantification of urban organic aerosols at a molecular level: identification, abundance and  
 1082 seasonal variation, *Atmos. Environ.*, 27(8), 1309–1330, [https://doi.org/10.1016/0960-](https://doi.org/10.1016/0960-1686(93)90257-Y)  
 1083 1686(93)90257-Y, 1993a.

- 1084 Rogge, W. F., Mazurek, M. A., Hildemann, L. M., Cass, G. R., and Simoneit, B. R. T.: Sources  
1085 of fine organic aerosol. 4. particulate abrasion products from leaf surfaces of urban plants,  
1086 *Environ. Sci. Technol.*, 27(13), 2700–2711, <https://doi.org/10.1021/es00049a008>, 1993b.
- 1087 Rosenfeld, D., Lohmann, U., Raga, G. B., O’Dowd, C. D., Kulmala, M., Fuzzi, S., Reissell,  
1088 A., and Andreae, M. O.: Flood or Drought: How Do Aerosols Affect Precipitation?, *Science*,  
1089 321(5894), 1309–1313, 2008.
- 1090 Samaké, A., Jaffrezo, J.-L., Favez, O., Weber, S., Jacob, V., Albinet, A., Riffault, V., Perdrix,  
1091 E., Waked, A., Golly, B., Salameh, D., Chevrier, F., Oliveira, D. M., Bonnaire, N., Besombes,  
1092 J.-L., Martins, J. M. F., Conil, S., Guillaud, G., Mesbah, B., Rocq, B., Robic, P.-Y., Hulin, A.,  
1093 Le Meur, S., Descheemaeker, M., Chretien, E., Marchand, N. and Uzu, G.: Polyols and  
1094 glucose particulate species as tracers of primary biogenic organic aerosols at 28 French sites,  
1095 *Atmos. Chem. Phys.*, 19(5), 3357–3374, <https://doi.org/10.5194/acp-19-3357-2019>, 2019a.
- 1096 Samaké, A., Jaffrezo, J.-L., Favez, O., Weber, S., Jacob, V., Albinet, A., Riffault, V., Perdrix, E.,  
1097 Waked, A., Golly, B., Salameh, D., Chevrier, F., Oliveira, D. M., Bonnaire, N., Besombes, J.-L.,  
1098 Martins, J. M. F., Conil, S., Guillaud, G., Mesbah, B., Rocq, B., Robic, P.-Y., Hulin, A., Le Meur,  
1099 S., Descheemaeker, M., Chretien, E., Marchand, N. and Uzu, G.: Polyols and glucose as tracers  
1100 of primary biogenic organic aerosol: influence of environmental factors on ambient air  
1101 concentrations and spatial distribution over France, *Atmos. Chem. Phys.*, [https://doi.org](https://doi.org/10.5194/acp-19-11013-2019)  
1102 [/10.5194/acp-19-11013-2019](https://doi.org/10.5194/acp-19-11013-2019), 2019b.
- 1103 Samaké, A., Bonin, A., Jaffrezo, J. L., Taberlet, P., Uzu, G., Jacob, V., Conil, S., and Martins,  
1104 J. M. F.: High levels of Primary Biogenic Organic Aerosols in the atmosphere in summer are  
1105 driven by only a few microorganisms from the leaves of surrounding plants, *Atmos. Chem.*  
1106 *Phys.*, <https://doi.org/10.5194/acp-20-5609-2020>, 2020.
- 1107 Samake, A., Martins, J. M., Bonin, A., Uzu, G., Taberlet, P., Conil, S., Favez, O., Thomasson,  
1108 A., Chazeau, B., Marchand, N., and Jaffrezo, J. L.: Variability of the atmospheric PM<sub>10</sub>  
1109 microbiome in three climatic regions of France, *Frontiers in Microbiology*, [https://doi.org](https://doi.org/10.3389/fmicb.2020.576750)  
1110 [10.3389/fmicb.2020.576750](https://doi.org/10.3389/fmicb.2020.576750), 2021.
- 1111 Sánchez-Ochoa, A., Kasper-Giebl, A., Puxbaum, H., Gelencsér, A., Legrand, M., and Pio, C.:  
1112 Concentration of atmospheric cellulose: A proxy for plant debris across a west-east transect  
1113 over Europe, *J. Geophys. Res.*, 112, <https://doi.org/10.1029/2006JD008180>, 2007.
- 1114 Simoneit, B. R. T., and Mazurek, M. A.: Organic matter of the troposphere—II. Natural  
1115 background of biogenic lipid matter in aerosols over the rural western united states, *Atmos.*  
1116 *Environ.*, 16(9), 2139–2159, [https://doi.org/10.1016/0004-6981\(82\)90284-0](https://doi.org/10.1016/0004-6981(82)90284-0), 1982.
- 1117 Schmidl, C.: PM<sub>10</sub>—Quellenprofile von Holzrauchemissionen aus Kleinf Feuerungen,  
1118 Diplomarbeit, Inst. für Chem. Technol. und Analytik, Tech. Univ. Wien, Vienna, 2005.
- 1119 Verma, S. K., Kawamura, K., Chen, J., and Fu, P.: Thirteen years of observations on primary  
1120 sugars and sugar alcohols over remote Chichijima Island in the western North Pacific, *Atmos.*  
1121 *Chem. Phys.*, 18(1), 81–101, 2018.

- 1122 Waked, A., Favez, O., Alleman, L. Y., Piot, C., Petit, J.-E., Delaunay, T., Verlinden, E., Golly,  
1123 B., Besombes, J.-L., Jaffrezo, J.-L., and Leoz-Garziandia, E.: Source apportionment of PM<sub>10</sub>  
1124 in a north-western Europe regional urban background site (Lens, France) using positive matrix  
1125 factorization and including primary biogenic emissions, *Atmos. Chem. Phys.*, 14(7), 3325–  
1126 3346, 2014.
- 1127 Wagenbrenner, N. S., Chung, S. H., and Lamb, B. K.: A large source of dust missing in  
1128 Particulate Matter emission inventories? Wind erosion of post-fire landscapes, *Elem. Sci.*  
1129 *Anth.*, 5(2), <https://doi.org/10.1525/elementa.185>, 2017.
- 1130 Weber, S., Salameh, D., Albinet, A., Alleman, L. Y., Waked, A., Besombes, J.-L., Jacob, V.,  
1131 Guillaud, G., Meshbah, B., Rocq, B., Hulin, A., Dominik-Sègue, M., Chrétien, E., Jaffrezo, J.-  
1132 L. and Favez, O.: Comparison of PM<sub>10</sub> Sources Profiles at 15 French Sites Using a  
1133 Harmonized Constrained Positive Matrix Factorization Approach, *Atmosphere*, 10(6), 310,  
1134 <https://doi.org/10.3390/atmos10060310>, 2019.
- 1135 Winiwarter, W., Bauer, H., Caseiro, A., and Puxbaum, H.: Quantifying emissions of primary  
1136 biological aerosol particle mass in Europe, *Atmos. Environ.*, 43, 1403–1409, 2009.
- 1137 Wu, C. and Yu, J. Z.: Determination of primary combustion source organic carbon-to-  
1138 elemental carbon (OC/EC) ratio using ambient OC and EC measurements: secondary OC-EC  
1139 correlation minimization method, *Atmos. Chem. Phys.*, 16, 5453–5465, 2016.
- 1140 Yttri, K. E., Aas, W., Bjerke, A., Cape, J. N., Cavalli, F., Ceburnis, D., Dye, C., Emblico, L.,  
1141 Facchini, M. C., Forster, C., Hanssen, J. E., Hansson, H. C., Jennings, S. G., Maenhaut, W.,  
1142 Putaud, J. P., and Tørseth, K.: Elemental and organic carbon in PM<sub>10</sub>: a one year  
1143 measurement campaign within the European Monitoring and Evaluation Programme EMEP,  
1144 *Atmos. Chem. Phys.*, 7, 5711–5725, <https://doi.org/10.5194/acp-7-5711-2007>, 2007.
- 1145 Yttri, K. E., Simpson, D., Stenström, K., Puxbaum, H. and Svendby, T.: Source apportionment  
1146 of the carbonaceous aerosol in Norway – quantitative estimates based on <sup>14</sup>C, thermal-optical  
1147 and organic tracer analysis, *Atmos. Chem. Phys. Discuss.*, 11(3), 7375–7422, 2011a.
- 1148 Yttri, K. E., Simpson, D., Nøjgaard, J. K., Kristensen, K., Genberg, J., Stenström, K.,  
1149 Swietlicki, E., Hillamo, R., Aurela, M., Bauer, H., Offenberg, J. H., Jaoui, M., Dye, C.,  
1150 Eckhardt, S., Burkhardt, J. F., Stohl, A., and Glasius, M.: Source apportionment of the summer  
1151 time carbonaceous aerosol at Nordic rural background sites, *Atmos. Chem. Phys.*, 11, 13339 –  
1152 13357, 2011b.
- 1153 Zhang, T., Engling, G., Chan, C. Y., Zhang, Y. N., Zhang, Z. S., Lin, M., Sang, X. F., Li, Y.  
1154 D., and Li, Y. S.: Contribution of fungal spores to particulate matter in a tropical rainforest,  
1155 *Environ. Res. Lett.*, 5(2), 24010, 2010.
- 1156 Zhu, C., Kawamura, K., and Kunwar, B.: Organic tracers of primary biological aerosol  
1157 particles at subtropical Okinawa Island in the western North Pacific Rim: Organic biomarkers  
1158 in the north pacific, *J. Geophys. Res. Atmospheres*, 120(11), 5504–5523, 2015.